Molecular Therapy
Nucleic Acids
Original Article

Modulation of the IL-6-Signaling Pathway in Liver Cells by miRNAs Targeting gp130, JAK1, and/or STAT3

Florence A. Servais,[1] Mélanie Kirchmeyer,[1] Matthias Hamdorf,[1,3] Nadège W.E. Minoungou,[1] Stefan Rose-John,[2] Stephanie Kreis,[1] Claude Haan,[1] and Iris Behrmann[1]

[1]Signal Transduction Laboratory, Life Sciences Research Unit, University of Luxembourg, 6, Avenue du Swing, 4367 Belvaux, Luxembourg; [2]Institute of Biochemistry, Christian-Albrechts-Universität zu Kiel, Medical Faculty, Olshausenstraße 40, 24098 Kiel, Germany

Interleukin-6 (IL-6)-type cytokines share the common receptor glycoprotein 130 (gp130), which activates a signaling cascade involving Janus kinases (JAKs) and signal transducer and activator of transcription (STAT) transcription factors. IL-6 and/or its signaling pathway is often deregulated in diseases, such as chronic liver diseases and cancer. Thus, the identification of compounds inhibiting this pathway is of interest for future targeted therapies. We established novel cellular screening systems based on a STAT-responsive reporter gene (*Cypridina luciferase*). Of a library containing 538 microRNA (miRNA) mimics, several miRNAs affected hyper-IL-6-induced luciferase activities. When focusing on candidate miRNAs specifically targeting 3′ UTRs of signaling molecules of this pathway, we identified, e.g., miR-3677-5p as a novel miRNA affecting protein expression of both STAT3 and JAK1, whereas miR-16-1-3p, miR-4473, and miR-520f-3p reduced gp130 surface expression. Interestingly, combination treatment with 2 or 3 miRNAs targeting gp130 or different signaling molecules of the pathway did not increase the inhibitory effects on phospho-STAT3 levels and STAT3 target gene expression compared to treatment with single mimics. Taken together, we identified a set of miRNAs of potential therapeutic value for cancer and inflammatory diseases, which directly target the expression of molecules within the IL-6-signaling pathway and can dampen inflammatory signal transduction.

INTRODUCTION

The inflammatory cytokine interleukin-6 (IL-6) signals via a receptor complex consisting of IL6R (IL6Rα, gp80) and the signaling subunit glycoprotein 130 (gp130) (IL6Rβ, IL6ST), shared among all IL-6-type cytokines. gp130-associated Janus kinase 1 (JAK1) phosphorylates different tyrosine residues in the cytoplasmic tail of gp130, to which mainly signal transducer and activator of transcription 3 (STAT3) transcription factors are recruited. Upon phosphorylation, STATs translocate into the nucleus and regulate the expression of various genes, including the one encoding suppressor of cytokine signaling 3 (SOCS3), an important negative regulator of this pathway.[1] Next to this classical signaling pathway triggered by membrane IL6R-gp130 complexes, IL-6 can also act on cells, which do not express IL6R (but only gp130) when complexed to a soluble form of IL6R (sIL6R), a process termed trans-signaling.[2]

In addition to its manifold physiological roles, e.g., in the immune system and in liver regeneration,[3,4] IL-6 has important systemic and local effects in the pathogenesis of cancers, such as multiple myeloma, endometrial cancer, lung cancer, colorectal cancer, renal cell carcinoma, cervical cancer, breast cancer, and ovarian carcinoma.[5,6] IL-6 is important for tumor development and angiogenesis, affecting the proliferation, migration, and invasion of cells, as well as for protecting them against drug treatments and apoptosis.[5,6] Tumor-induced systemic IL-6 can induce systemic metabolic changes, e.g., lipolysis in the white adipose tissue and insulin resistance of the skeletal muscle, which may ultimately lead to cancer inflammation-induced cachexia (reviewed in White[7]). In addition, IL-6 can act locally in the tumor on immune cells to suppress anti-cancer immunity.[8,9] For example, IL-6 favors the development of M2 macrophages and myeloid-derived suppressor cells (MDSCs), leading to increased levels of immunosuppressive factors such as IL-10 and IL-4, while it attenuates the differentiation of Th1 cells. Tumor-associated macrophages have also been described to produce IL-6, thus promoting the expansion of hepatocellular carcinoma (HCC) stem cells and, therefore, tumorigenesis.[10]

IL-6 plays an important role in HCC, the focus of this study. IL-6 and sIL6R levels have been shown to be increased in the sera of patients with HCC,[11] and high levels of serum IL-6 can serve as a biomarker for an elevated risk to develop HCC.[12] Increased activity of STAT3 was observed in liver tumors of mice treated with N-nitrosodiethylamine (DEN);[13] later, IL-6 was found to be crucially implicated in this HCC mouse model,[14,15] which, according to gene expression

Received 21 December 2018; accepted 24 March 2019;
https://doi.org/10.1016/j.omtn.2019.03.007.

[3]Present address: Terasaki Research Institute, 11570 W. Olympic Blvd., Los Angeles, CA 90064, USA

Correspondence: Iris Behrmann, Signal Transduction Laboratory, Life Sciences Research Unit, University of Luxembourg, 6, Avenue du Swing, 4367 Belvaux, Luxembourg.
E-mail: iris.behrmann@uni.lu

data, best resembles liver cancer with poor prognosis in humans.[16] Autocrine production of IL-6 by liver cancer progenitor cells also contributes to their malignant progression.[17] While liver-specific knockout of SOCS3 promoted DEN-induced hepatocarcinogenesis,[18,19] deletion of gp130 or STAT3 reduced HCC prevalence and resulted in smaller tumors in DEN-treated mice.[15,20] Similarly, in another chemically induced HCC mouse model (thioacetamide based), the absence of STAT3 in liver parenchymal cells attenuated HCC development.[21] Interestingly, IL-6-trans-signaling, rather than classical signaling, seems to be responsible for DEN-dependent tumor development.[22,23] Of note, a whole-genome sequencing study of 88 matched pairs of (hepatitis B virus [HBV]-related) HCC tumor and surrounding tissues indicated that the (IL-6)-JAK-STAT-signaling pathway is a major oncogenic driver in HCC, with mutations in almost half of the cases investigated, including *IL6R* gene amplifications in 26% of the samples and (in part, gain-of-function) mutations in the *JAK1* gene in 9.1%.[24]

Altogether, these data strongly suggest an important role of IL-6 signaling in the initiation and development of HCC, and they have spawned the interest of targeting molecules involved in the IL-6-JAK-STAT3-signaling pathway as a strategy to block STAT3 activation.[25–27] Compounds targeting IL-6-STAT3 signaling have been reported to suppress the transformed phenotype and tumor progression.[5,6] For example, treatment with antisense oligonucleotides (ASOs) targeting STAT3 leads to an inhibition of proliferation of various hepatoma cell lines, a reduction of tumor size, and an improved survival of mice bearing orthotopically xenografted HCC.[28] Interestingly, STAT3 ASO therapy has entered clinical trials, yielding the first promising results particularly for the treatment of lymphoma and lung cancer.[29] Other studies on hepatoma describe stronger effects of anti-cancer drugs when this pathway is concomitantly targeted, pointing at the anti-apoptotic effects of JAK-STAT3 signaling and its implication in drug resistance.[26,30]

MicroRNAs (miRNAs) have been recognized as promising drug candidates (miRNA replacement therapy) as well as drug targets (e.g., of anti-miRNAs), and nucleic acid-based therapeutic approaches are particularly promising if the target organ is the liver.[31–33] Therefore, we aimed to identify miRNAs that can modulate the IL-6-JAK1-STAT3-signaling pathway in hepatoma cells. To do so, we established 2 novel functional cellular screening systems, which allowed for the selection of miRNAs affecting expression of STAT3-responsive reporter genes. Of a library of 538 mimics, we identified a set of miRNAs targeting 3′ UTR sequences of the main signaling molecules of the pathway. Further characterization revealed their effects on STAT3 or JAK1 protein expression, on gp130 surface availability, as well as on cytokine-mediated signaling events.

RESULTS

Two Novel Cellular High-Throughput Screening Systems Identify Candidate miRNAs as Modulators of the IL-6-JAK-STAT3-Signaling Pathway

To identify miRNAs that regulate the IL-6-JAK-STAT3-signaling pathway, we first performed a pre-screen of a miRNA mimic-based library in HEK293T reporter cells (whose growth is not affected by IL-6 signaling), engineered to express the secreted *Cypridina luciferase* gene under the control of 6 (synthetic) STAT3-responsive elements (see Figure S1 for a schematic flowchart of this study). Since sIL6R is known to be upregulated in HCC and IL-6 trans-signaling has been implied in HCC,[11,23] we stimulated the cells with hyper-IL-6 (hy-IL-6) to detect miRNAs, which modulate the signaling independently of the membrane-bound IL6R (hy-IL-6 is a designer cytokine composed of sIL6R linked to IL-6[34]).

From 538 molecules tested (see Table S1), 129 miRNA candidates, which either increased or decreased luciferase activity without a major effect on growth (data not shown), were retained for the screen in the hepatoma cell line Hep3B. The latter was engineered to express the secreted *Cypridina luciferase* gene under the control of a highly IL-6-inducible STAT3-specific rat pancreatitis-associated protein 1 (rPAP1) promoter[35,36] (Figure S2). miRNA candidates were selected based on a reduction or increase in the luciferase activity, normalized to the negative control mimic (NMC) as well as to the viability of the Hep3B reporter cells (Figure S3; it should be noted that hy-IL-6 does not stimulate Hep3B cell proliferation). Based on this analysis, 34 miRNA mimics were selected to be further studied regarding their ability to modulate phosphorylation and, thus, activation of STAT3. These included miR-124-3p and miR-142-3p, previously shown to target molecules involved in the JAK-STAT pathway (STAT3,[37] IL6R,[38] and gp130,[39] respectively), thus serving as positive controls.

Effect of Selected miRNAs on Endogenous pSTAT3 and STAT3 Levels following Cytokine Stimulation

In the previous screening approaches, miRNA candidates were identified, which affected the IL-6-signaling cascade. To further refine this list of interesting miRNAs, the phosphorylation of STAT3 (as functional readout) and total STAT3 (as potential target) were quantified by western blot analysis in Hep3B cells transfected with each of the 34 miRNA mimics and stimulated with hy-IL-6 (Figure 1). miR-142-3p, a miRNA known to target gp130, the common signaling receptor for all IL-6-type cytokines, only slightly decreased phosphorylated (p) STAT3 and STAT3 levels (Figure 1). The other control, miR-124-3p, reduced the expression level of STAT3 by 50%, as previously published,[37] but it had no effect on pSTAT3, in line with the finding that only a part of STAT3 proteins generally becomes phosphorylated following cytokine stimulation.[40] Based on their potential to reduce pSTAT3 and/or STAT3 levels, 15 candidate miRNAs were selected for the identification of their putative target(s) by luciferase-3′ UTR reporter assays (in bold and marked with a star, Figure 1; some candidates, such as miR-155-5p, were not taken along as they have been extensively studied;[41] see also Figure 6).

Identification of miRNA Mimics Reducing gp130 Surface Availability

Next, we were interested to screen for miRNAs that specifically and directly target gp130. To do so, luciferase reporter assays were performed using plasmids harboring the cDNA for *Gaussia luciferase*, a secreted enzyme, followed by 3′ UTR sequences of gp130. As the

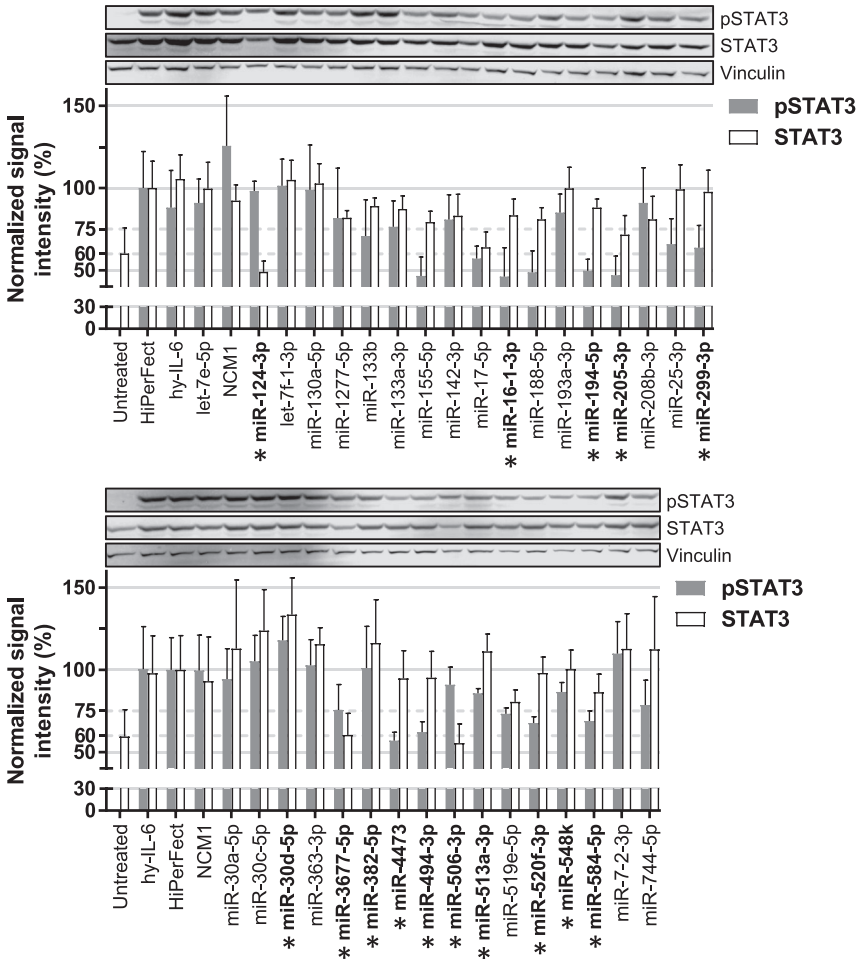

Figure 1. Effect of Selected miRNAs on STAT3 and pSTAT3 Protein Levels

Hep3B cells were transfected with 34 selected mimics and 2 days later stimulated for 24 h with hy-IL-6 to activate the JAK-STAT pathway. pSTAT3 and STAT3 protein levels were quantified using the LI-COR device and normalized to total protein staining (data not shown). The normalized signal obtained for each sample was divided by the signal obtained for the transfection control (HiPerFect). Vinculin staining is shown as an additional control. Error bars represent the SD of 3 biological replicates. Mimics selected for luciferase-3′ UTR reporter assays are in bold and marked with a star. A representative western blot result for pSTAT3, STAT3, and Vinculin is shown.

3′ UTR of the gene encoding gp130 is very long (6,001 bp), 3 different plasmids with separate, overlapping parts of the gp130 3′ UTR were constructed (Figure 2A). HEK293T cells were used for the co-transfection experiments as they can be better transfected than liver-derived cells, thereby providing a smaller variability between the biological replicates.

After a first, preliminary experiment with all 15 miRNA candidates (data not shown), 10 were further evaluated for their binding to the gp130 3′ UTR sequence: miR-16-1-3p, miR-205-3p, miR-4473, and miR-520f-3p reproducibly decreased the luciferase activity of the respective gp130 3′ UTR plasmid by more than 50% (gp130a, Figure 2B). Similarly, miR-194-5p and miR-584-5p as well as miR-382-5p and miR-4473 reduced the luciferase activity of the plasmids harboring the part b or c, respectively, by at least 40% (Figure 2B). No off-target effects of these miRNA mimics were found in control experiments using only the backbone vector (Figure S4). In total, 7 different miRNA mimics (miR-16-1-3p, miR-194-5p, miR-205-3p, miR-382-5p, miR-4473, miR-520f-3p, and miR-584-5p, depicted in gray in Figure 2B) had a strong effect on gp130 3′ UTR.

As IL-6 (classical or trans-) signaling is initiated from gp130 receptors present at the plasma membrane, we evaluated the effects of selected miRNAs on the surface expression of endogenous gp130 by flow cytometry in different cell lines from various tissues. In comparison to the cells transfected with NCM1 (in gray), miR-16-1-3p, miR-194-5p, miR-4473, and miR-520f-3p decreased gp130 surface expression in both Hep3B hepatoma cells (Figure 2C) and non-transformed PH5CH8 liver cells (Figure 2D). Two miRNAs had cell-specific effects: miR-382-5p reduced gp130 surface expression only in Hep3B cells, while miR-584-5p affected gp130 surface expression (relative to the NCM1 control) only in PH5CH8 cells (Figures S5A and S5B). Finally, miR-205-3p had almost no effects on the gp130 levels in both tested liver cell lines (Figures S5A and S5B), although it had clear effects in the reporter gene assays.

miR-16-1-3p, miR-4473, and miR-520f-3p were further tested in a variety of other cells types, such as lung adenocarcinoma (A549), prostate carcinoma (DU145), HEK293T, and melanoma cells (IGR39). Upon transfection of each miRNA tested (orange), histograms were strongly shifted to the left in comparison to control cells (Figures 2E–2H), indicating that these 3 miRNAs have a robust effect on the surface expression of gp130 in a variety of cells.

miR-16-1-3p, miR-4473, and miR-520f-3p Inhibit hy-IL-6-Inducible Phosphorylation of STAT3 and Differentially Affect the Expression of a Target Gene

Surface availability of gp130 has been shown to regulate the cell responsiveness to IL-6-type cytokines. For example, gp130 expression is downregulated during granulocyte differentiation[42] and upon activation of T cells.[43] Moreover, pre-stimulation with IL-1β reduces gp130 availability at the surface of human hepatocytes[44] or monocytes[45] in a p38-dependent manner. Therefore,

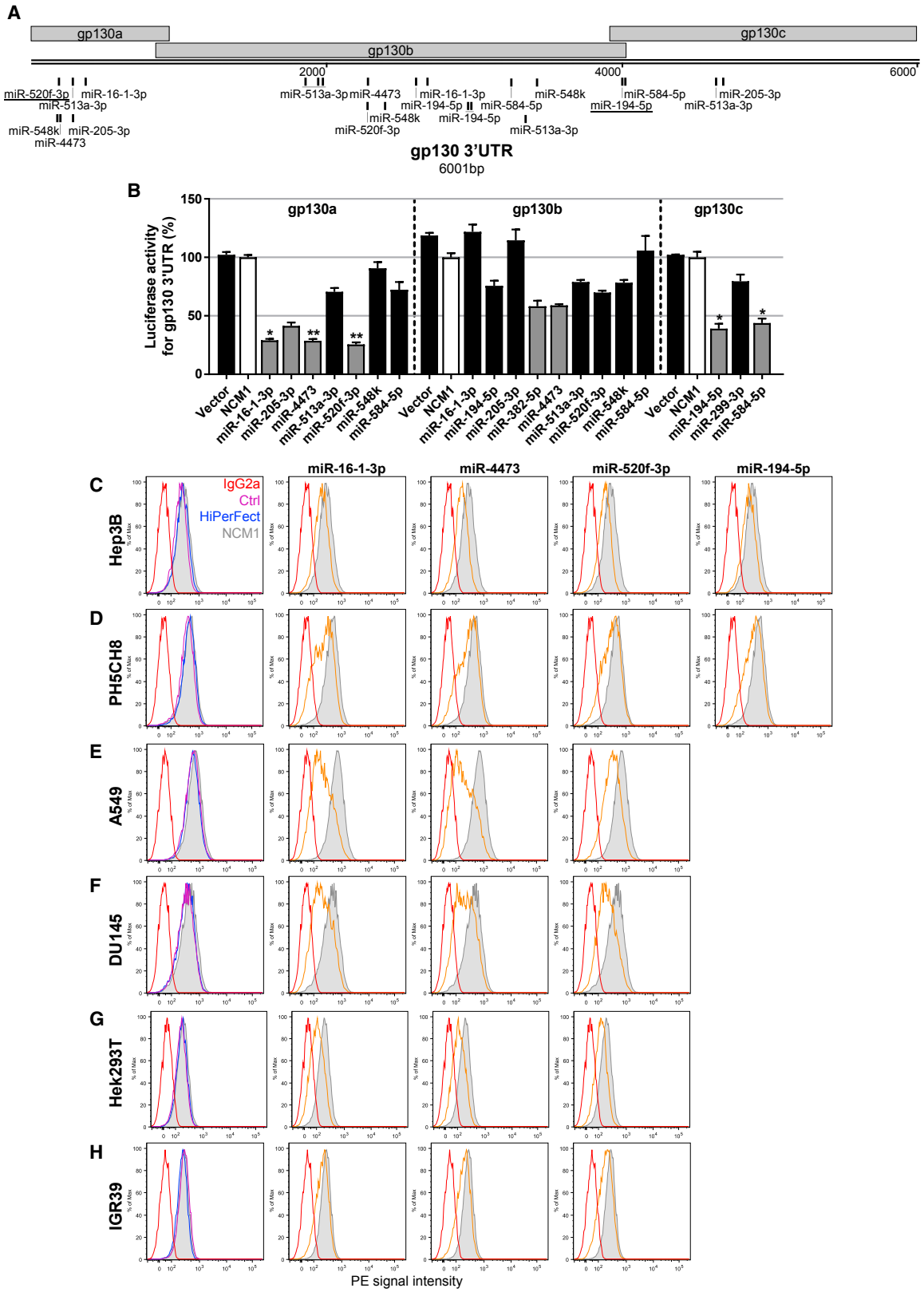

(legend on next page)

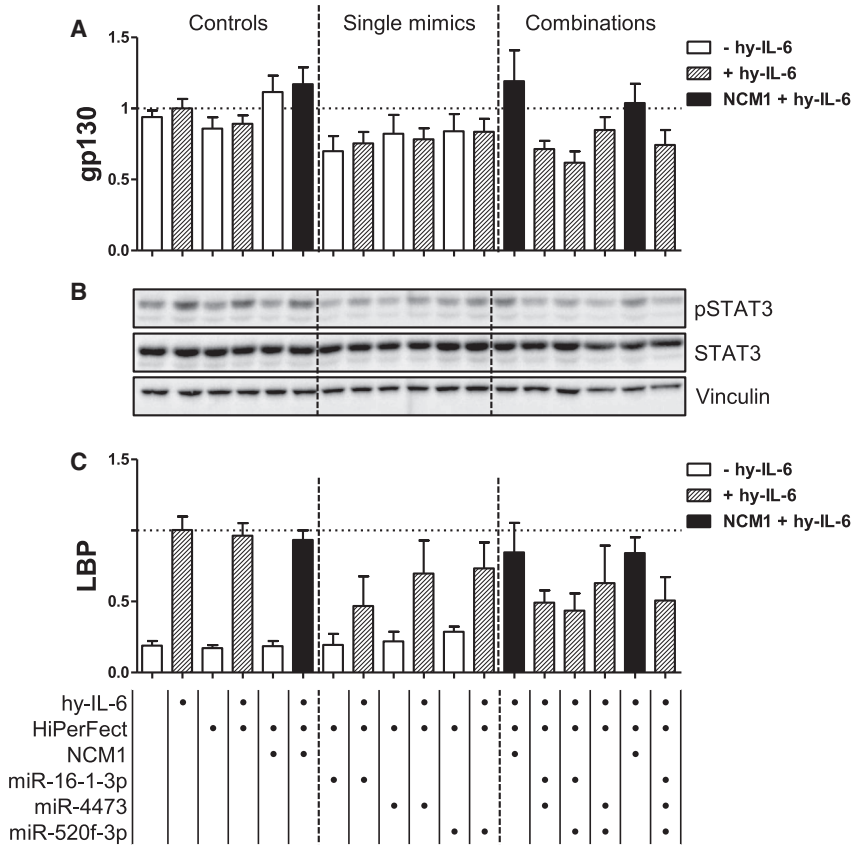

Figure 3. miR-16-1-3p, miR-4473, and miR-520f-3p Partially Prevent the Activation of STAT3 upon hy-IL-6 Stimulation by Targeting gp130 mRNA, Reducing the Expression of a hy-IL-6 Target Gene in PH5CH8 Cells

Cells were left untreated, reverse transfected with NCM1 or miR-16-1-3p, miR-4473, and miR-520f-3p mimics (20 nM), and were stimulated with hy-IL-6 (20 ng/mL). Single mimics as well as combinations were tested and compared to the respective NCM1 control (in black). For the double or triple combinations, 40 or 60 nM NCM1 was used as the respective control. (A) Normalized mRNA expression level of gp130. (B) Representative western blot analysis of both the activated and total forms of STAT3 and of the Vinculin as loading control. (C) Normalized mRNA expression level of *Lipopolysaccharide-binding protein* (LBP). The mRNA levels were monitored upon mimic transfection and hy-IL-6 stimulation (depicted with dashed lines). Error bars represent the SD of at least 3 biological replicates. Bottom indicates the applied treatments per lane.

we investigated if the effects of miR-16-1-3p, miR-4473, and miR-520f-3p on gp130 were sufficient to modulate the activation of STAT3 upon hy-IL-6 stimulation. First of all, we confirmed that the corresponding miRNA expression level was indeed increased upon mimic transfection (Figure S6). An only slightly suppressive effect of the 3 miRNA mimics on gp130 mRNA expression was observed (Figure 3A), suggesting that translational repression, rather than mRNA decay, may substantially contribute to gp130 downregulation (for a review, see Iwakawa and Tomari[46]). Interestingly, all 3 miRNA mimics largely reduced inducible STAT3 phosphorylation in comparison to the NCM1, whereas STAT3 protein levels remained unchanged (single mimics, Figure 3B). The basal level of STAT3 phosphorylation (i.e., without stimulation) was not affected by any of the 3 mimics (or combinations thereof), indicating that this "tonic" STAT3 phosphorylation may be mediated by signaling events independent of gp130 (e.g., elicited by growth factors or non-IL-6-type cytokines).

To further address the impact of these miRNAs on a signaling readout, we monitored their effect on the inducibility of *Lipopolysaccharide-binding protein* (LBP), a target gene of IL-6 signaling.[47] All 3 miRNAs reduced inducible LBP mRNA expression in PH5CH8 cells; the effect was strongest for miR-16-1-3p, with a reduction by more than 50% in comparison to the cytokine-stimulated control cells (Figure 3C). Combination of 2 or all 3 miRNAs had no additional effect than the one measured for miR-16-1-3p alone. Of note, miR-4473 and miR-520f-3p, which were less effective in dampening inducible LBP mRNA expression compared to miR-16-1-3p, also target the 3′ UTR of SOCS3, the major negative regulator of the pathway (Figure S7A).

Identification of miRNA Mimics Directly Targeting JAK1 and STAT3

In similar approaches, we also screened for miRNAs targeting JAK1 and STAT3, 2 other major players of the pathway. In luciferase-3′ UTR reporter assays, we identified 8 miRNA candidates (in gray, Figures 4A and 4C) to be further analyzed for their effects on endogenous

Figure 2. Identification of miRNAs Targeting the Co-receptor gp130 and Affecting Its Surface Availability

(A) Graphic representations of the gp130 3′ UTR as well as the predicted binding sites (based on TargetScan website). Sites conserved among mammals are underlined. (B) HEK293T cells were co-transfected with mimics specifically selected for one of the vectors harboring the *Gaussia luciferase* cDNA followed by overlapping 3′ UTR sequences of the gene encoding gp130 (gp130a/b/c). Mimics selected for further functional assays are shown in gray, and negative control mimic 1 (NCM1) is in white. Error bars represent the SD of 3 biological replicates. Kruskal-Wallis followed by Dunn's Post hoc test were performed to assess statistical significance represented with $*p < 0.05$ and $**p < 0.01$. (C–H) Selected miRNA candidates affect the surface availability of gp130 in various cell lines. (C) Hep3B hepatoma cells, (D) non-neoplastic PH5CH8 liver cells, (E) A549 lung adenocarcinoma cells, (F) DU145 prostate cancer cells, (G) HEK293T cells, and (H) IGR39 melanoma cells were either left untreated (Ctrl, in purple) or transfected with a negative control (NCM1, in gray) or one of the selected miRNA mimics and analyzed for gp130 surface expression level by flow cytometry. Candidate miRNAs are depicted in orange, the isotype control is in red, and the transfection control is in blue.

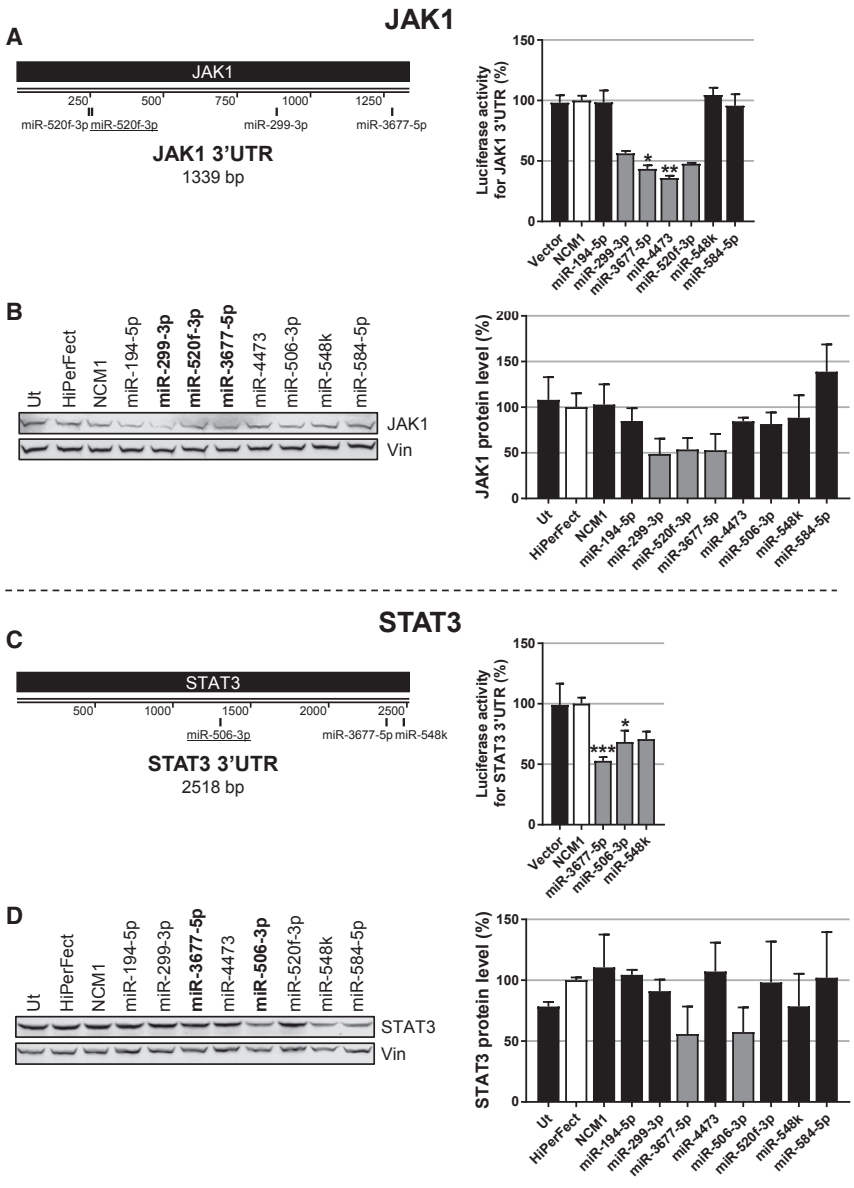

Figure 4. Identification of miRNAs Targeting JAK1 and STAT3 and Affecting Their Endogenous Protein Levels

(A and C) Graphic representations of (A) JAK1 and (C) STAT3 3′ UTRs as well as predicted binding sites (TargetScan). Sites conserved among mammals are underlined. HEK293T cells were co-transfected with the mimics specifically selected for each construct and one of the vectors harboring the *Gaussia luciferase* cDNA followed by the 3′ UTR of the gene encoding (A) JAK1 or (C) STAT3. Mimics selected for further functional assays are shown in gray, and NCM1 is in white. Kruskal-Wallis followed by Dunn's post hoc test were performed to assess statistical significance represented with *$p < 0.05$, **$p < 0.01$, and ***$p < 0.001$. (B and D) Selected miRNAs downregulate endogenous JAK1 and STAT3 protein levels in PH5CH8 cells. (B) miR-299-3p, miR-3677-5p, and miR-520f-3p reduce JAK1 protein levels. (D) miR-3677-5p and miR-506-3p reduce STAT3 protein levels. A representative western blot as well as quantifications are depicted. Error bars represent the SD of at least 3 biological replicates.

JAK1 and/or STAT3 protein levels. To do so, PH5CH8 cells were transfected with either NCM1 or one of the selected mimics (miR-194-3p, miR-299-3p, miR-3677-5p, miR-4473, miR-506-3p, miR-520f-3p, miR-548k, and miR-584-5p).

The 3′ UTR of the mRNA encoding JAK1 was found to be strongly targeted by miR-299-3p, miR-3677-5p, miR-4473, and miR-520f-3p (Figure 4A). Importantly, of these 4, 3 mimics (miR-299-3p, miR-520f-3p, and miR-3677-5p) also strongly decreased JAK1 protein level by approximately 50% (depicted in gray, Figure 4B), while miR-4473 only had a modest effect.

Regarding STAT3, miR-3677-5p, miR-506-3p, and miR-548k were identified as mimics targeting its 3′ UTR (Figure 4C). STAT3 protein levels in non-neoplastic PH5CH8 cells were reduced by ~50% upon transfection with miR-3677-5p and miR-506-3p (Figure 4D, depicted in gray). However, miR-548k had less impact on STAT3 protein expression (Figure 4D). Similar findings were observed previously in Hep3B hepatoma cells (Figure 1C).

Single Mimics Targeting Various Proteins of the IL-6-Signaling Pathway Attenuate IL-6-STAT3-Induced Gene Readouts as Effectively as Combination Treatments

As a next step, we tested whether a combination of miRNAs with different targets in the IL-6-signaling pathway would have stronger inhibitory effects on cytokine signaling compared to single mimics. For these combinatory experiments, we selected miR-16-1-3p, miR-299-3p, and miR-124-3p: miR-16-1-3p targets gp130, miR-299-3p targets JAK1 (and likely IL6R, see Figure S7B), and miR-124-3p targets STAT3 (and likely IL6R, see Figure S7B) (see Figure 6 for a summary). We now stimulated with IL-6 (and not with hy-IL-6) so that the potential effects of a lower IL6R expression would also be reflected in the results. In this context, we utilized Hep3B cells as they respond better to IL-6 stimulation than PH5CH8 cells (data not shown).

Figure S8 shows the controls for the efficient transfection of the mimics as well as their effects on the different target mRNAs. JAK1 mRNA expression was only affected by miR-299-3p; basal and IL-6-inducible expression of STAT3 mRNA was attenuated only by miR-124-3p. In contrast, expression of gp130 was affected not only by miR-16-1-3p (in line with the previous experiments) but also by miR-299-3p.

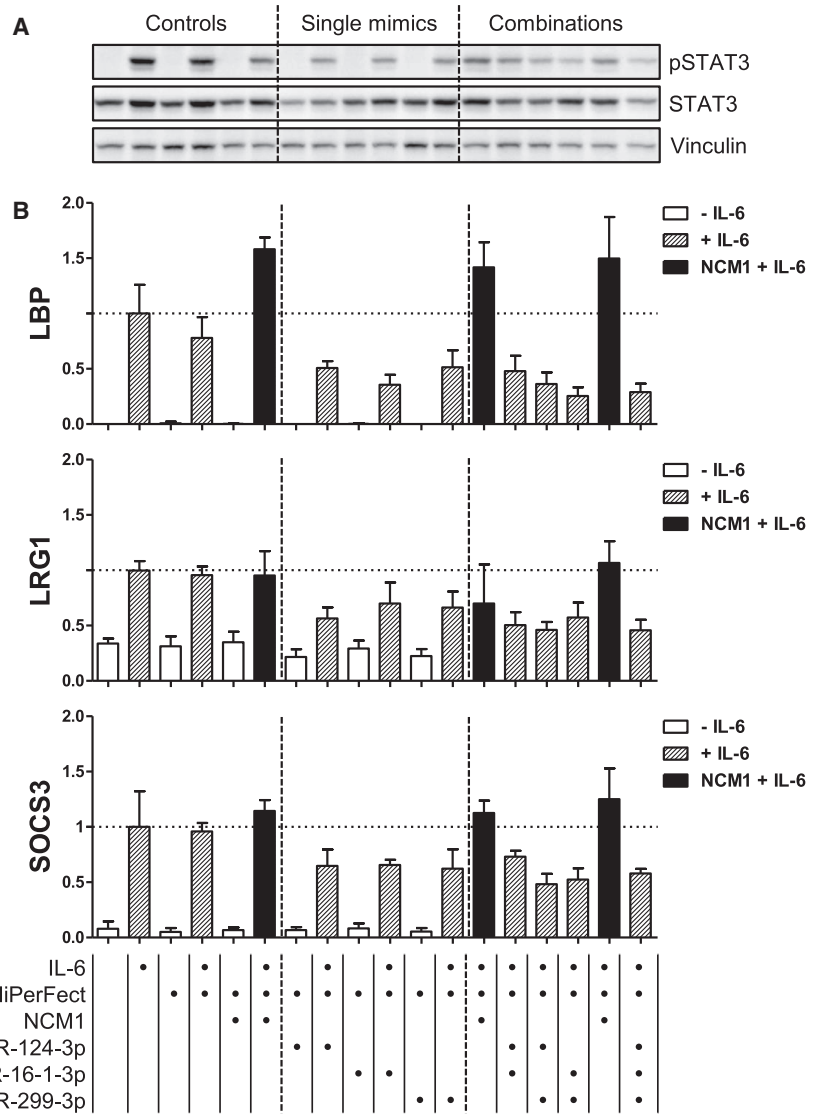

Figure 5. miR-124-3p, miR-16-1-3p, and miR-299-3p Partially Prevent the Activation of STAT3 upon IL-6 Stimulation by Targeting STAT3, IL6R, gp130, and JAK1 mRNA, and They Reduce the Induction of the Expression of IL-6 Target Genes in Hep3B Cells

Cells were left untreated, reverse transfected with NCM1 or miR-124-3p, miR-16-1-3p, and miR-299-3p mimics (20 nM), and stimulated with IL-6 (20 ng/mL). Single mimics as well as combinations were tested and compared to the respective NCM1 control (in black). For the double or triple combinations, 40 or 60 nM NCM1 was used as the respective control. (A) Western blot analysis for both the activated and total forms of STAT3 and of Vinculin as loading control. (B) Normalized mRNA expression levels of LBP, *Leucine-rich alpha-2 glycoprotein* (LRG1), and *SOCS3* were monitored upon mimic transfection and IL-6 stimulation (depicted with dashed lines). Error bars represent the SD of at least 3 biological replicates. Bottom indicates the applied treatments per lane.

Interestingly, IL6R mRNA expression was reduced by all 3 mimics, which was expected for miR-124-3p and miR-299-3p (see Figure S7B), but not for miR-16-1-3p (miR-299-3p and miR-16-1-3p had little effect in the preliminary experiment with reporter plasmids comprising 3′ UTR sequences of gp130 or IL6R, respectively; data not shown).

Clear inhibitory effects of all 3 miRNAs were observed for the activation of STAT3 (Figure 5A) as well as for the IL-6-inducible expression of the STAT3 target genes *LBP*, *Leucine-rich alpha-2 glycoprotein* (LRG1), and *SOCS3* (Figure 5B). Interestingly, combination treatments were not more effective than single treatments (Figure 5, combinations).

DISCUSSION

In this study, (1) we show that a screen of 538 miRNA mimics designed to identify miRNAs influencing IL-6 (trans-)signaling yielded a panel of interesting candidate miRNAs affecting the (hyper-)IL-6-gp130-JAK1-STAT3 pathway. (2) We validated several selected miRNAs by showing that they specifically interact with the 3′ UTR of the gp130, JAK1, and/or STAT3 mRNAs. (3) We confirmed some of those miRNAs to specifically affect the expression of different proteins in this pathway, notably, gp130, JAK1, and STAT3. (4) We found that treatment with single mimics was as effective in downregulating cytokine signaling as combinations of multiple miRNA mimics targeting either gp130 or various molecules in the IL-6-signaling pathway.

As described in the Introduction, IL-6 has important systemic and local effects in the pathogenesis of cancer. It influences tumor development, angiogenesis, cell proliferation, migration, and invasion; it has anti-apoptotic and immunomodulatory effects.[5,6] Previous studies have demonstrated miRNAs as regulators of the JAK-STAT-signaling pathway. For instance, miR-124 has been extensively studied and shown to target both STAT3[37] and IL6R.[38,48] Another example is miR-142-3p, which was shown to directly target the co-receptor gp130 in cardiac myocytes,[39] macrophages,[49] and endometrial stromal cells.[50]

The aim of this study was to identify miRNAs with the potential for inhibiting the IL-6-JAK-STAT3-signaling pathway and that, therefore, might be of therapeutic relevance. Although there are still issues with miRNA-based therapies (e.g., delivery, poor penetration in tissues, stability, off-target effects; reviewed in Chen),[51] the potential of nucleic acids as versatile drug candidates is more and more recognized.[32,33] For example, miRNA-based drugs have been successfully used in pre-clinical studies (e.g., miR-26[52] and anti-miR-17[53,54]) as well as in first clinical trials, such as for miR-16-based mimics.[55]

A

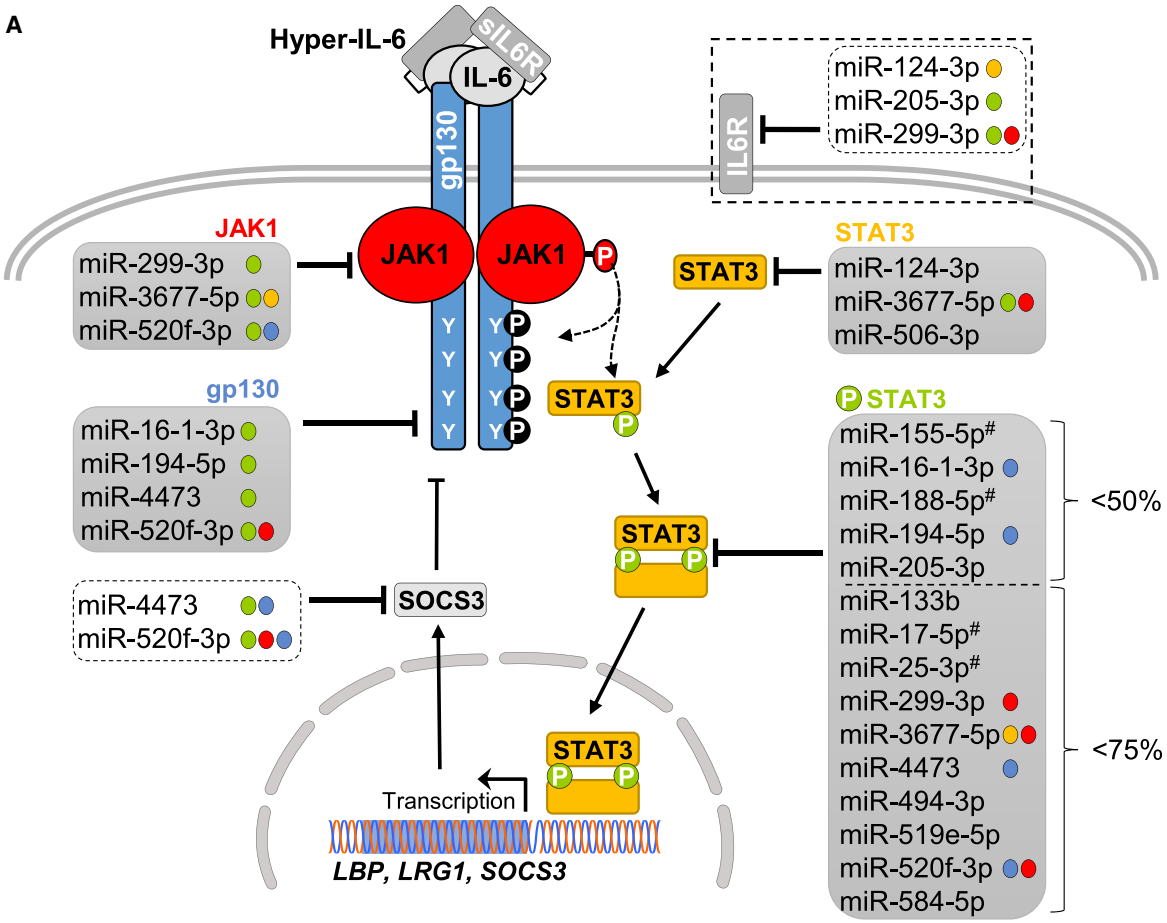

B

miRNA	Protein levels (Hep3B)				Protein levels (PH5CH8)						Luciferase-3'UTR (Hek293T)									
	pSTAT3		STAT3		STAT3		JAK1		gp130		STAT3		JAK1		gp130		IL6R		SOCS3	
	% to Ctrl	SD	% to Ctrl	SD	% to Ctrl	SD	% to Ctrl	SD	% to Ctrl	SD	% to Ctrl	SD	% to Ctrl	SD	% to Ctrl	SD	% to Ctrl	SD	% to Ctrl	SD
miR-16-1-3p	46	18	83	9	-	-	-	-	52	11	-	-	-	-	29	1	-	-	-	-
miR-205-3p	47	12	71	11	-	-	-	-	83	27	-	-	-	-	41	3	57	12	-	-
miR-194-5p	50	7	88	4	104	4	85	14	68	12	-	-	98	10	39	4	-	-	-	-
miR-4473	57	5	94	14	107	24	85	4	69	6	-	-	36	2	29	1	-	-	58	5
miR-494-3p	62	6	95	13	-	-	-	-	-	-	No target identified									
miR-299-3p	64	14	98	13	91	10	49	17	-	-	-	-	56	2	80	6	36	3	109	13
miR-520f-3p	68	4	98	7	98	34	54	12	69	11	-	-	48	1	26	2	84	2	50	7
miR-584-5p	69	6	86	9	102	37	139	30	65	17	-	-	96	9	44	4	-	-	99	6
miR-3677-5p	76	16	60	12	56	23	53	18	-	-	53	3	43	3	-	-	-	-	-	-
miR-513a-3p	86	3	111	9	-	-	-	-	-	-	-	-	-	-	71	3	75	16	-	-
miR-548k	87	6	100	9	79	27	88	25	-	-	71	6	105	6	78	2	-	-	117	5
miR-506-3p	91	11	55	11	57	20	82	13	-	-	68	9	-	-	-	-	88	9	-	-
miR-124-3p	98	6	49	7	-	-	-	-	-	-	-	-	-	-	-	-	63	3	-	-
miR-382-5p	101	25	116	23	-	-	-	-	79	18	-	-	-	-	58	5	-	-	-	-
miR-30d-5p	118	15	134	26	-	-	-	-	-	-	-	-	-	-	-	-	-	-	82	4

Figure 6. Summary of the Results Obtained in This Study

(A) Graphical overview of effects of the different miRNA mimics on the IL-6-type cytokine-signaling pathway. For STAT3 phosphorylation, the mimics that reduce the western blot signal to below 75% or below 50% are listed. For JAK1 and STAT3 mimics, those that reduce the western blot signal to below 60% are shown. For gp130, the mimics that reduce surface expression efficiently (below 70%) are listed. The colored dots behind the name of the mimics in the lists indicate additional target genes of the respective miRNA (red, JAK1; blue, gp130; yellow, STAT3; and green, phosphorylation of STAT3). miRNAs labeled with a "#" have already been characterized before. Interestingly, downregulation of STAT3 protein alone was never associated with a reduction of phosphorylated STAT3. (B) Summary of the results obtained upon transfection with each of

(legend continued on next page)

Here we describe and characterize the effects of several novel miRNAs and of some previously described ones (e.g., miR-124-3p and miR-506-3p) on the IL-6-signaling pathway (see Figure 6). We focused on miRNAs that did not affect cell viability, but it would also be very interesting to further investigate those miRNAs that alter cellular viability, as previously done for cholangiocarcinoma.[56] For example, the miR-374 family, from which 3 of 6 members were included in the large library and led to an enhanced cell proliferation (data not shown), has already been associated with an increased proliferation and survival, e.g., in gastrointestinal stromal tumors,[57] gastric cancer,[58] and hepatoma.[59]

miRNA-Mediated Effects on STAT3

Interestingly, we noticed that among those miRNAs that most strongly reduced STAT3 protein levels (miR-124-3p, miR-3677-5p, and miR-506-3p), only miR-3677-5p reduced pSTAT3 signals (Figure 1). miR-3677-5p was found to also target JAK1 (see below), which may explain that this miRNA is more effective on STAT3 phosphorylation than the others. Our results indicate that a reduction of STAT3 levels by 50% does not translate into decreased pSTAT3 levels. Indeed, only a fraction of STAT3 is phosphorylated upon IL-6 stimulation.[40] A certain reduction in the expression can thereby be tolerated without a necessary effect on the absolute amounts of pSTAT3.

Another interesting aspect of STAT3 silencing is that, in the absence of STAT3, IL-6 leads to a sustained STAT1 activation[60] and switches to an interferon (IFN)γ-like response in hepatoma cells.[61] IFNγ is one of those cytokines long known to be involved in anti-tumor defense, since interferon gamma receptor (IFNγR) and STAT1 deficiency has been described to increase cancer susceptibility upon treatment with chemical pathogens in mice.[62,63] Of note, the observed reduction of STAT3 expression (by 50%) is not only insufficient to reduce the phosphorylation of STAT3 but also not able to induce a compensatory phosphorylation of STAT1 (data not shown).

In contrast to our first findings (Figure 1), several studies have observed a decrease of pSTAT3 signals by miR-124-3p.[37,38,48] However, it needs to be taken into consideration that this miRNA also targets IL6R (seen also in our hands in the luciferase-3′ UTR assay [Figure S7B] and confirmed at the mRNA levels [Figure S8]), which can translate into a reduced signaling input when analyzing signals elicited by IL-6 (as observed in our final experiment utilizing IL-6 as a stimulating cytokine; Figure 5). Since we used the designer cytokine hy-IL-6 for the first experiments, the observed signaling effects were independent of the surface level of IL6R.

miRNA-Mediated Effects on JAK1

miRNA-mediated downregulation of JAK1 in cancer has been shown to suppress metastasis and invasion (e.g., miR-214 in lung carcinoma,[64] miR-340 in HCC,[65] and miR-488 in pancreatic ductal adenocarcinoma[66]). We found the 3 miRNAs miR-299-3p, miR-3677-5p, and miR-520f-3p to diminish JAK1 protein levels by at least 40%. While JAK1 knockdown only partially inhibits IL-6 signaling, expression of kinase-deficient mutants of JAK1 totally abolishes IL-6 signaling (unpublished data), indicating that the partial signaling reduction in the knockdown scenario is due to compensatory binding of the other JAKs (JAK2 or Tyk2) to gp130. Thus, even a very efficient downregulation of JAK1 by a miRNA is unlikely to have drastic effects on IL-6 signaling.

In addition, the downregulation of JAK1 is likely to impact on a variety of other cytokine signals, as JAK1 is the most promiscuous Janus kinase from the 4 family members. It is used for the signaling of the majority of the ~40 cytokine receptors. For instance, IFNα/β, IFNγ, and IL-27 signaling, all associated with anti-tumor functions, are concomitantly reduced when JAK1 is downregulated.[61] Interferon-mediated antiviral responses have already been shown to be impaired by miRNAs targeting JAK1 (e.g., miR-30c[67] and miR-373[68]). Therefore, it needs to be evaluated whether an inhibition of JAK1 would be useful in a tumor situation, as IFNs essentially have anti-tumor effects.[69] On the other hand, these miRNAs may be useful to diminish inflammatory processes involving both IFNs and IL-6-type cytokines. Similarly, due to their strong anti-inflammatory effects, JAK inhibitors are regarded as highly promising in inflammatory diseases.[70]

miR-299-3p was shown to target the 3′ UTR of JAK1 and to efficiently suppress JAK1 mRNA and protein expression (Figures S8C and 4B). Interestingly, it also affected the 3′ UTR of the IL6R (Figure S7B). Known targets of miR-299-3p include vascular endothelial growth factor A (VEGFA),[71,72] androgen receptor,[73] and ATP Binding Cassette Subfamily E Member 1 (ABCE1),[74] which have been linked to tumor-suppressive functions (less angiogenesis, viability, or drug resistance). Moreover, miR-299-3p has been shown to be downregulated in The Cancer Genome Atlas (TCGA) HCC tumor samples and to inhibit growth and invasion of SK-HEP-1 hepatoma cells.[75]

We also identified miR-3677-5p as a novel miRNA involved in the regulation of the JAK-STAT pathway. Interestingly, it targets the expression of both STAT3 and JAK1 with poorly conserved binding sites present in their 3′ UTRs (Figures 4A and 4C). Overexpression of miR-3677-5p reduces mRNA and protein levels of STAT3 and JAK1 in Hep3B and Huh-7 hepatoma cells as well as in non-neoplastic PH5CH8 cells (Figures 1 and 4; data not shown). Very little

the 15 selected miRNAs for pSTAT3 (Figure 1, Hep3B), JAK1, and STAT3 (Figure 4, PH5CH8) protein levels, for gp130 surface availability (Figure S5, PH5CH8) and for luciferase-3′ UTR reporter assays (Figures 2, 4, and S7, HEK293T). Results represent the protein and luciferase signals measured for the corresponding target compared to the control (expressed in %). The SD of at least 3 biological replicates is shown. A dash indicates that no data were obtained for this specific miRNA and target. For miR-494-3p, no target could be identified from the ones tested. The list of miRNA effects is colorcoded for the protein levels in Hep3B and PH5CH8 cells (reduction depicted in red and increase in green). In addition, the miRNAs are sorted according to their inhibitory effects on STAT3 activation (from the strongest to the lowest).

is known about this miRNA. In contrast to most other miRNAs discussed here, which are associated with tumor-suppressive functions, miR-3677-5p is upregulated in HCC and an increased expression correlates with poor survival,[76,77] indicating a potential tumor-promoting role. Of note, however, this is one of the very few miRNAs showing divergent effects in the 2 reporter cell lines: while it reduced luciferase activity in the Hep3B reporter cells, it increased reporter gene activity in the first screen in Hek-293T reporter cells (see Table S2). Clearly, this miRNA warrants further analysis.

miRNA-Mediated Effects on gp130

Finally, we identified miRNAs efficiently decreasing gp130 surface expression. miR-16-1-3p, miR-4477, miR-520f-3p, and miR-194-5p showed a reduction of at least 25% of gp130 surface expression. As gp130 is the signaling receptor shared by the IL-6-type cytokines, these miRNAs may be particularly relevant in situations requiring the inhibition of various cytokines of the IL-6 family. Indeed, monotherapies with monoclonal antibodies targeting IL-6 or IL6R have failed in clinical trials against multiple myeloma,[78–80] metastatic renal cell carcinoma,[81] and prostate cancer,[82,83] probably due to the compensation of the IL-6-signaling pathway by other gp130 ligands.[84,85]

One of the miRNAs identified here to target gp130 was also reducing JAK1 protein levels (miR-520f-3p). Interestingly, 2 of the miRNAs efficiently reducing gp130 surface availability (miR-16-1-3p and miR-194-5p) caused a strong reduction of phosphorylated STAT3 (suppression of greater than 50%; Figure 1). The 2 other miRNAs (miR-4473 and miR-520f-3p) only reduced pSTAT3 levels at least 25% compared to the control. miR-4473 and miR-520f-3p were also less potent than miR-16-1-3p when monitoring the effects on *LBP* expression, a STAT3-inducible gene (Figure 3C). Interestingly, those 2 miRNAs also bound to SOCS3 3′ UTR (Figure S7A), the major inhibitor of IL-6 signaling, which might explain their overall weaker effect. A careful comparison with the effects of small interfering RNAs (siRNAs) specifically downregulating their target mRNAs would allow for a further dissection of the impact of "other" miRNA targets on the signaling readouts. However, in order to facilitate this comparison, doses of siRNAs would have to be adjusted to achieve only partially suppressed levels similar to the ones obtained with miRNAs.

miR-16-1-3p is part of a well-characterized tumor suppressor cluster (*mir-15a∼16-1*, reviewed in Huang),[86] located in the chromosomal region 13q14.2, which is often deleted in cancer.[87–90] Interestingly, min-icells loaded with miR-16-based mimics (TargomiRs) have entered first clinical trials for patients with malignant mesothelioma.[55] While many targets have been identified for miR-16-5p, its passenger strand is less studied. Recently, it was shown to target TWIST1 in gastric[91] and non-small-cell lung[92] cancer cells. To our knowledge, no link between miR-16-1-3p and the IL-6-JAK-STAT3-signaling pathway had been established so far.

miRNAs affecting the receptor availability may be particularly promising candidates for further investigation (see Figure 6B), and they will have more specific effects than miRNAs targeting signaling molecules shared by many cytokines. Notably, several of the miRNAs identified to affect IL-6 signal transduction have actually multiple targets within the pathway (see Figure 6). Combinations of miRNAs, either sharing the same target (gp130; Figure 3) or regulating different signaling molecules of the pathway (gp130, JAK1, STAT3, and/or IL6R; Figure 5) did not increase effects compared to single treatments, indicating that drug candidates based on a single miRNA might be able to achieve optimal signal attenuation. However, possible saturation effects need to be addressed by detailed dose-response analyses (we used up to 60-nM mimics for the combination treatments shown in Figures 3 and 5; for comparison, Liang et al.[93] described that transfection of 10-fold less siRNA already led to considerable AGO2 competition of endogenous miRNAs). A more detailed analysis of miRNA cooperation may also be warranted, considering that the spacing between two miRNAs on the 3′ UTR of a common target mRNA may contribute to the efficiency of target mRNA downregulation. Saetrom et al.[94] have determined the optimal spacing for downregulation to be between 17 and 35 nt between the seed sites.

Subsequent studies will have to evaluate the therapeutic relevance of selected miRNAs on cellular behavior (proliferation, migration, and invasion) as well as in the context of IL-6-dependent disease models, in particular for inflammatory diseases (e.g., rheumatoid arthritis) and cancer (e.g., HCC).

MATERIALS AND METHODS

Materials and Cell Culture

All cells were grown at 37°C in a water-saturated atmosphere at 5%C CO_2. HEK293T, Hep3B, PH5CH8, and DU145 cells were maintained in DMEM (Lonza, Basel, Switzerland) and A549 cells in DMEM-F12 medium (Lonza, Basel, Switzerland), both supplemented with 10% fetal bovine serum (FBS) (Gibco, Thermo Fisher Scientific, Erembodegem, Belgium), 25 mM HEPES (Lonza, Basel, Switzerland), and 100 μg/mL normocin (InvivoGen, Toulouse, France). IGR39 cells were cultured in RPMI 1640 medium (Lonza, Basel, Switzerland) supplemented with 10% FBS and 100 μg/mL normocin.

All miRIDIAN miRNA mimics were obtained from Dharmacon (GE Healthcare, Diegem, Belgium). Vectors containing the 3′ UTR sequence of the genes coding for IL6R (GenBank: NM_181359.1), gp130 (GenBank: NM_001190981.1), JAK1 (GenBank: NM_002227.2), SOCS3 (GenBank: NM_003955.4), and STAT3 (GenBank: NM_213662.1) were purchased from GeneCopoeia (Tebu-Bio, Boechout, Belgium), as well as the backbone vector (pEZX-MT05) is used as a control to monitor the off-target effects. Mimic transfections were performed using HiPerFect Transfection Reagent (QIAGEN, Venlo, the Netherlands) and 20 nM miRNA mimic (or control), according to the manufacturer's instructions. Co-transfections of 3′ UTR reporter vectors and miRNA mimics were performed using DharmaFect Duo (Dharmacon, GE Healthcare, Diegem, Belgium), 100 ng 3′ UTR reporter vector, and 20 nM miRNA mimic (or control), according to the manufacturer's protocol.

2 days after mimic transfection, cells were stimulated for 24 h with 20 ng/mL hy-IL-6, a designer cytokine comprising IL-6 bound to the extracellular domain of IL6R (sIL6R) through a flexible polypeptide linker.[34] For Figure 5, Hep3B cells were stimulated with 20 ng/mL IL-6 (PeproTech, Tebu-Bio, Boechout, Belgium) instead of hy-IL-6.

Engineering of Stable Cell Lines Allowing for High-Throughput Screening of miRNAs Affecting the JAK-STAT(3)-Signaling Pathway

HEK293T cells were plated in 6-well plates in complete medium, and, 24 h later, they were transduced with lentiviral particles containing 6 STAT3-responsive elements (STAT3-REs, sequence: 5-TTCTGGGAA-3′), followed by a minimal cytomegalovirus (CMV) promoter in front of the secreted *Cypridina luciferase* gene and linked to a puromycin resistance gene. 48 h after transduction, selection of transduced cells was initiated with 3 μg/mL puromycin (InvivoGen, Toulouse, France). After several rounds of selection, hy-IL-6 responsiveness of the construct was assessed by measuring the Cypridina luciferase activity in the supernatant of stimulated HEK293T-STAT3-RE-Cypridina luciferase (Cluc) cells (20 ng/mL hy-IL-6). The transfected clone showing the highest fold induction of luciferase activity upon cytokine treatment was selected and amplified.

Hep3B cells (hepatoma cells with a ploidy status of n = 3.2, see Wilkens et al.[95]; for mutations in cancer genes see Table S1 in Ewald)[96] were plated in 6-well plates in complete medium and transfected with a linearized plasmid containing the STAT3-inducible promoter rPAP1[35,36] in front of the secreted *Cypridina luciferase* gene, using the PromoFectin-Hepatocyte reagent (PromoCell, Bio-Connect, Huissen, the Netherlands), following the manufacturer's protocol. 4 h later, serum-reduced Optim-MEM medium (Life Technologies, Merelbeke, Belgium) was replaced by normal DMEM. After 4 days, selection of transfected cells was initiated with 500 μg/mL G418 (Sigma-Aldrich, Diegem, Belgium). After several rounds of selection, a pool of Hep3B-rPAP1-Cluc cells was tested for successful inducible luciferase production and secretion upon stimulation with 20 ng/mL hy-IL-6 (Figure S2B) and amplified.

Selection of miRNAs for the Pre-screen

We designed a library consisting of 538 miRNAs, which were selected from miRBase version (v.)21 by the following criteria: (1) presence in the high-confidence list from miRBase,[97] (2) predicted by Diana web server v.5.0[98,99] to target molecule(s) related to IL-6 signaling, (3) presence in the top 100 list of miRNAs regulated upon hy-IL-6 stimulation in primary hepatocytes (microarray analysis, ArrayExpress: E-MTAB-6572),[100] and (4) miRNAs previously published as regulated by STAT3 (for a complete list, see Table S1).

Luciferase Reporter Gene Assays

For the miRNA library screens, 10^4 HEK293T-STAT3-RE-Cluc or Hep3B-rPAP1-Cluc engineered cells were reverse transfected on a 96-well plate with 20 nM of the respective miRIDIAN miRNA mimic using HiPerFect Transfection Reagent (QIAGEN, Venlo, the Netherlands). 48 h after transfection, cells were stimulated for 24 h, as described in the figure legends, after which supernatants were collected and kept at −20°C until measurement. Briefly, 10 μL supernatant was used to measure the secreted Cypridina luciferase activity using the BioLux Cypridina Luciferase assay kit (New England Biolabs, Bioke, Leiden, the Netherlands), following the manufacturer's instructions. Automatic injection of substrate and measurement were performed with the CLARIOstar plate reader (BMG Labtech, ISOGEN Life Science, De Meern, the Netherlands).

For the identification of IL6R, gp130, JAK1, SOCS3, and STAT3 as potential target(s) of selected miRNA mimics, 10^4 HEK293T cells were plated on a 96-well plate and co-transfected the next day with a mimic and either the backbone vector or a vector containing the *Gaussia luciferase* gene followed by (a portion of) the 3′ UTR sequence of IL6R (IL6Ra or b), gp130 (gp130a, b, or c), JAK1, SOCS3, or STAT3. After 2 days of transfection, cell supernatants were collected to assess the activities of both the secreted Gaussia luciferase and the secreted Alkaline phosphatase, used for normalization purposes, using the Secrete-pair dual luminescence assay kit (GeneCopoeia, Tebu-Bio, Boechout, Belgium), according to the manufacturer's protocol. Both activities were determined with the CLARIOstar plate reader. For all luciferase experiments, at least 3 independent biological replicates, each with 3 technical replicates, were performed.

Cell Viability Assessment

To monitor the effects of the miRNA mimics on cell growth (and thereby reduce false-positive results), cell viability was assessed for the same wells as the luciferase measurements using the PrestoBlue reagent (Invitrogen, Thermo Fisher Scientific, Erembodegem, Belgium), according to the manufacturer's instructions. The fluorescence of each well was then measured with the CLARIOstar plate reader and normalized to the fluorescence emitted by the cells treated with HiPerFect transfection reagent only, present on each plate.

Flow Cytometry

The effects of miRNA mimics on gp130 receptors were assessed by flow cytometry. Briefly, transfected cells were resuspended in cold PBS supplemented with 5% FBS and 0.1% sodium azide (Sigma-Aldrich, Diegem, Belgium) and incubated with 0.5 μg antibody against gp130 (555757, BD Biosciences, Erembodegem, Belgium) or the corresponding isotype control antibody, immunoglobulin G (IgG)2α (21225021, Immunotools, Friesoythe, Germany), for 1 h at 4°C. Cells were then washed with cold PBS-azide and incubated with secondary labeled antibodies (715-116-150, Jackson ImmunoResearch Laboratories, Bio-Connect, Huissen, the Netherlands). After 1 h of incubation at 4°C, cells were again washed with cold PBS-azide and then analyzed on a FACSCanto II flow cytometer using the FACSDiva software (BD Biosciences, Erembodegem, Belgium). Overlay plots were created using the FlowJo software (FlowJo, Ashland, OR).

Cell Lysis and Western Blot Analysis

Cultured cells were lysed on the plate with ice-cold Laemmli 1× buffer and kept at −20°C. Before separation by SDS-PAGE and blotting either onto a polyvinylidene fluoride (PVDF)-PSQ (for LI-COR) or a PVDF-FL (for enhanced chemiluminescence [ECL]) membrane (Millipore, Overijse, Belgium), protein extracts were heated for 10 min at 96°C. Blots were incubated overnight with antibodies against human JAK1 (610232, BD Biosciences, Erembodegem, Belgium), STAT3 (610189, BD Biosciences, Erembodegem, Belgium), pSTAT3 (9145, Cell Signaling Technology, Bioke, Leiden, the Netherlands), or Vinculin (13901, Cell Signaling Technology, Bioke, Leiden, the Netherlands). After washing, membranes were incubated for 1 h at room temperature with either fluorescent (LI-COR Biosciences, Westburg, Leusden, the Netherlands) or horseradish peroxidase (HRP)-conjugated secondary antibodies (Cell Signaling Technology, Bioke, Leiden, the Netherlands) for LI-COR or ECL detection, respectively. Prior to ECL detection, membranes were incubated in an ECL solution containing 2.5 mM luminol, 2.6 mM hydrogen peroxide, 100 mM Tris/HCl (pH 8.8), and 0.2 mM paracoumaric acid.[101] Signals were detected with the Odyssey classic (LI-COR Biosciences, Westburg, Leusden, the Netherlands) or Fusion SL device (Vilber, Analis, Suarlee, Belgium). Protein levels were quantified by using the Image Studio Lite software (version 5.2, LI-COR Biosciences, Lincoln, NE) and normalized to the total protein content (REVERT Total Protein Stain, LI-COR Biosciences, Westburg, Leusden, the Netherlands), following the manufacturer's instructions.

Total RNA Isolation and qPCR

Total RNA was extracted using the Quick-RNA MiniPrep Kit (Zymo Research, Laborimpex, Brussels, Belgium) and reverse transcribed with the miScript II RT kit (QIAGEN, Venlo, the Netherlands) in a volume of 10 μL, according to the respective manufacturer's instructions. Real-time qPCR was carried out on a CFX384 Detection System (Bio-Rad, Temse, Belgium), using 5- or 50-ng (miRNA or mRNA detection, respectively) RNA input in a 10-μL reaction volume, 2× iTaq SYBR Green Supermix (Bio-Rad, Temse, Belgium), and 1 μL 10× miRNA-specific primers (QIAGEN, Venlo, the Netherlands) or either 2.5 pmol gene-specific primer pairs or 1 μL 10× QuantiTech primers (QIAGEN, Venlo, Netherlands). miRNAs and mRNAs of interest, as well as small RNAs used as miRNA normalizers (RNU1A, SCARNA17, and SNORD95) and reference genes used for RNA normalization (HRPT, PPIA, and TBP), were assessed in parallel for each sample and run in triplicates. Calculations were carried out by using the CFX Manager software (Bio-Rad, Temse, Belgium) provided with the machine.

Primers were purchased from Eurogentec (Liège, Belgium) and the sequences were as follows: IL6R forward, 5′-GTATTCCCAGGAGTCCCAGA-3′; IL6R reverse, 5′-GCAAGATTCCACAACCCTG-3′; gp130 forward, 5′-TGAAACTGCTGTGAATGTGG-3′; gp130 reverse, 5′-CATCCTTCCCACCTTCATCT-3′; HPRT forward, 5′-TGGACAGGACTGAACGTCTT-3′; HPRT reverse, 5′-GAGCACACAGAGGGCTACAA-3′; JAK1 forward, 5′-TCTTGGAATCCAGTGGAGGCATAAA-3′; JAK1 reverse, 5′-CACTCTTCCCGGATCTTGTTTTTCT-3′; LBP forward, 5′-AGGTGATGTTTAAGGGTGAAAT-3′; LBP reverse, 5′-ATAATCCGAGATGGCAAAGTA-3′; PPIA forward, 5′-CAGACAAGGTCCCAAAGACA-3′; PPIA reverse, 5′-CCATTATGGCGTGTGAAGTC-3′; SOCS3 forward, 5′-ATGAGAACTGCCAGGGAATC-3′; SOCS3 reverse, 5′-CCCAGGCTCCACAACCA-3′; STAT3 forward, 5′-ACACAGATAAACTTGGTCTTCAGGTA-3′; STAT3 reverse, 5′-GCCAGAGAGCCAGGAGCA-3′; TBP forward, 5′-ACCCAGCAGCATCACTGTT-3′; and TBP reverse, 5′-CGCTGGAACTCGTCTCACTA-3′.

Statistical Analysis

Statistical significance between control (NCM1) and the candidate miRNA for western blot analysis (Figures 1 and 4) and luciferase assays (Figures 2, 4, S4, and S7) was assessed by non-parametric one-way ANOVA (Kruskal-Wallis test), followed by Dunn's multiple comparisons test performed with the statistical program Prism 7 (GraphPad, La Jolla, CA, USA).

SUPPLEMENTAL INFORMATION

Supplemental Information can be found online at https://doi.org/10.1016/j.omtn.2019.03.007.

AUTHOR CONTRIBUTIONS

Conceptualization, C.H., S.K., and I.B.; Methodology, F.A.S., M.K., and I.B.; Investigation, F.A.S., M.K., N.W.E.M., and M.H.; Resources, S.R.-J.; Writing – Original Draft, F.A.S., C.H., and I.B.; Writing – Review & Editing, F.A.S., C.H., S.K., and I.B.; Supervision, S.K., and I.B.; Funding Acquisition, C.H., S.K., and I.B.

CONFLICTS OF INTEREST

The authors declare no competing interests.

ACKNOWLEDGMENTS

This work was funded by the Luxembourg National Research Fund (FNR) and the Deutsche Forschungsgemeinschaft (C12/BM/3975937, Inter project "HepmiRSTAT"), by the FNR funding scheme PRIDE (Doctoral Training Unit CANBIO, project number 10675146), and by the Internal Research Project «IL6LongLiv» of the University of Luxembourg. We are grateful to Professor Nobuyuki Kato, Okayama University, Japan, for providing the PH5CH8 cells. We thank Demetra Philippidou, Catherine Rolvering, Sébastien Plançon, Odile Lecha, Aurélien Ginolhac, and Eric Koncina for helpful technical advice. We thank Michèle Gaetti for the work performed during her master thesis in our research group.

REFERENCES

1. Heinrich, P.C., Behrmann, I., Haan, S., Hermanns, H.M., Müller-Newen, G., and Schaper, F. (2003). Principles of interleukin (IL)-6-type cytokine signalling and its regulation. Biochem. J. *374*, 1–20.
2. Rose-John, S. (2012). IL-6 trans-signaling via the soluble IL-6 receptor: importance for the pro-inflammatory activities of IL-6. Int. J. Biol. Sci. *8*, 1237–1247.
3. Taub, R. (2004). Liver regeneration: from myth to mechanism. Nat. Rev. Mol. Cell Biol. *5*, 836–847.
4. Tanaka, T., Narazaki, M., and Kishimoto, T. (2014). IL-6 in inflammation, immunity, and disease. Cold Spring Harb. Perspect. Biol. *6*, a016295.

5. Guo, Y., Xu, F., Lu, T., Duan, Z., and Zhang, Z. (2012). Interleukin-6 signaling pathway in targeted therapy for cancer. Cancer Treat. Rev. *38*, 904–910.
6. Johnson, D.E., O'Keefe, R.A., and Grandis, J.R. (2018). Targeting the IL-6/JAK/STAT3 signalling axis in cancer. Nat. Rev. Clin. Oncol. *15*, 234–248.
7. White, J.P. (2017). IL-6, cancer and cachexia: metabolic dysfunction creates the perfect storm. Transl. Cancer Res. *6* (*Suppl 2*), S280–S285.
8. Burkholder, B., Huang, R.-Y., Burgess, R., Luo, S., Jones, V.S., Zhang, W., Lv, Z.Q., Gao, C.Y., Wang, B.L., Zhang, Y.M., and Huang, R.P. (2014). Tumor-induced perturbations of cytokines and immune cell networks. Biochim. Biophys. Acta *1845*, 182–201.
9. Tsukamoto, H., Fujieda, K., Senju, S., Ikeda, T., Oshiumi, H., and Nishimura, Y. (2018). Immune-suppressive effects of interleukin-6 on T-cell-mediated anti-tumor immunity. Cancer Sci. *109*, 523–530.
10. Wan, S., Zhao, E., Kryczek, I., Vatan, L., Sadovskaya, A., Ludema, G., Simeone, D.M., Zou, W., and Welling, T.H. (2014). Tumor-associated macrophages produce interleukin 6 and signal via STAT3 to promote expansion of human hepatocellular carcinoma stem cells. Gastroenterology *147*, 1393–1404.
11. Soresi, M., Giannitrapani, L., D'Antona, F., Florena, A.M., La Spada, E., Terranova, A., Cervello, M., D'Alessandro, N., and Montalto, G. (2006). Interleukin-6 and its soluble receptor in patients with liver cirrhosis and hepatocellular carcinoma. World J. Gastroenterol. *12*, 2563–2568.
12. Aleksandrova, K., Boeing, H., Nöthlings, U., Jenab, M., Fedirko, V., Kaaks, R., Lukanova, A., Trichopoulou, A., Trichopoulos, D., Boffetta, P., et al. (2014). Inflammatory and metabolic biomarkers and risk of liver and biliary tract cancer. Hepatology *60*, 858–871.
13. Sánchez, A., Nagy, P., and Thorgeirsson, S.S. (2003). STAT-3 activity in chemically-induced hepatocellular carcinoma. Eur. J. Cancer *39*, 2093–2098.
14. Naugler, W.E., Sakurai, T., Kim, S., Maeda, S., Kim, K., Elsharkawy, A.M., and Karin, M. (2007). Gender disparity in liver cancer due to sex differences in MyD88-dependent IL-6 production. Science *317*, 121–124.
15. He, G., Yu, G.Y., Temkin, V., Ogata, H., Kuntzen, C., Sakurai, T., Sieghart, W., Peck-Radosavljevic, M., Leffert, H.L., and Karin, M. (2010). Hepatocyte IKKbeta/NF-kappaB inhibits tumor promotion and progression by preventing oxidative stress-driven STAT3 activation. Cancer Cell *17*, 286–297.
16. Lee, J.S., Grisham, J.W., and Thorgeirsson, S.S. (2005). Comparative functional genomics for identifying models of human cancer. Carcinogenesis *26*, 1013–1020.
17. He, G., Dhar, D., Nakagawa, H., Font-Burgada, J., Ogata, H., Jiang, Y., Shalapour, S., Seki, E., Yost, S.E., Jepsen, K., et al. (2013). Identification of liver cancer progenitors whose malignant progression depends on autocrine IL-6 signaling. Cell *155*, 384–396.
18. Ogata, H., Kobayashi, T., Chinen, T., Takaki, H., Sanada, T., Minoda, Y., Koga, K., Takaesu, G., Maehara, Y., Iida, M., and Yoshimura, A. (2006). Deletion of the SOCS3 gene in liver parenchymal cells promotes hepatitis-induced hepatocarcinogenesis. Gastroenterology *131*, 179–193.
19. Riehle, K.J., Campbell, J.S., McMahan, R.S., Johnson, M.M., Beyer, R.P., Bammler, T.K., and Fausto, N. (2008). Regulation of liver regeneration and hepatocarcinogenesis by suppressor of cytokine signaling 3. J. Exp. Med. *205*, 91–103.
20. Hatting, M., Spannbauer, M., Peng, J., Al Masaoudi, M., Sellge, G., Nevzorova, Y.A., Gassler, N., Liedtke, C., Cubero, F.J., and Trautwein, C. (2015). Lack of gp130 expression in hepatocytes attenuates tumor progression in the DEN model. Cell Death Dis. *6*, e1667.
21. Abe, M., Yoshida, T., Akiba, J., Ikezono, Y., Wada, F., Masuda, A., Sakaue, T., Tanaka, T., Iwamoto, H., Nakamura, T., et al. (2017). STAT3 deficiency prevents hepatocarcinogenesis and promotes biliary proliferation in thioacetamide-induced liver injury. World J. Gastroenterol. *23*, 6833–6844.
22. Hong, J., Wang, H., Shen, G., Lin, D., Lin, Y., Ye, N., Guo, Y., Li, Q., Ye, N., Deng, C., and Meng, C. (2016). Recombinant soluble gp130 protein reduces DEN-induced primary hepatocellular carcinoma in mice. Sci. Rep. *6*, 24397.
23. Bergmann, J., Müller, M., Baumann, N., Reichert, M., Heneweer, C., Bolik, J., Lücke, K., Gruber, S., Carambia, A., Boretius, S., et al. (2017). IL-6 trans-signaling is essential for the development of hepatocellular carcinoma in mice. Hepatology *65*, 89–103.
24. Kan, Z., Zheng, H., Liu, X., Li, S., Barber, T.D., Gong, Z., Gao, H., Hao, K., Willard, M.D., Xu, J., et al. (2013). Whole-genome sequencing identifies recurrent mutations in hepatocellular carcinoma. Genome Res. *23*, 1422–1433.
25. Schust, J., Sperl, B., Hollis, A., Mayer, T.U., and Berg, T. (2006). Stattic: a small-molecule inhibitor of STAT3 activation and dimerization. Chem. Biol. *13*, 1235–1242.
26. Liu, Y., Li, P.K., Li, C., and Lin, J. (2010). Inhibition of STAT3 signaling blocks the anti-apoptotic activity of IL-6 in human liver cancer cells. J. Biol. Chem. *285*, 27429–27439.
27. Moser, C., Lang, S.A., Mori, A., Hellerbrand, C., Schlitt, H.J., Geissler, E.K., Fogler, W.E., and Stoeltzing, O. (2008). ENMD-1198, a novel tubulin-binding agent reduces HIF-1alpha and STAT3 activity in human hepatocellular carcinoma(HCC) cells, and inhibits growth and vascularization in vivo. BMC Cancer *8*, 206.
28. Li, W.C., Ye, S.L., Sun, R.X., Liu, Y.K., Tang, Z.Y., Kim, Y., Karras, J.G., and Zhang, H. (2006). Inhibition of growth and metastasis of human hepatocellular carcinoma by antisense oligonucleotide targeting signal transducer and activator of transcription 3. Clin. Cancer Res. *12*, 7140–7148.
29. Hong, D., Kurzrock, R., Kim, Y., Woessner, R., Younes, A., Nemunaitis, J., Fowler, N., Zhou, T., Schmidt, J., Jo, M., et al. (2015). AZD9150, a next-generation antisense oligonucleotide inhibitor of STAT3 with early evidence of clinical activity in lymphoma and lung cancer. Sci. Transl. Med. *7*, 314ra185.
30. Xie, L., Zeng, Y., Dai, Z., He, W., Ke, H., Lin, Q., Chen, Y., Bu, J., Lin, D., and Zheng, M. (2018). Chemical and genetic inhibition of STAT3 sensitizes hepatocellular carcinoma cells to sorafenib induced cell death. Int. J. Biol. Sci. *14*, 577–585.
31. Lorenzer, C., Dirin, M., Winkler, A.M., Baumann, V., and Winkler, J. (2015). Going beyond the liver: progress and challenges of targeted delivery of siRNA therapeutics. J. Control. Release *203*, 1–15.
32. Hosseinahli, N., Aghapour, M., Duijf, P.H.G., and Baradaran, B. (2018). Treating cancer with microRNA replacement therapy: A literature review. J. Cell. Physiol. *233*, 5574–5588.
33. Shen, X., and Corey, D.R. (2018). Chemistry, mechanism and clinical status of antisense oligonucleotides and duplex RNAs. Nucleic Acids Res. *46*, 1584–1600.
34. Fischer, M., Goldschmitt, J., Peschel, C., Brakenhoff, J.P., Kallen, K.J., Wollmer, A., Grötzinger, J., and Rose-John, S. (1997). I. A bioactive designer cytokine for human hematopoietic progenitor cell expansion. Nat. Biotechnol. *15*, 142–145.
35. Dusetti, N.J., Ortiz, E.M., Mallo, G.V., Dagorn, J.C., and Iovanna, J.L. (1995). Pancreatitis-associated protein I (PAP I), an acute phase protein induced by cytokines. Identification of two functional interleukin-6 response elements in the rat PAP I promoter region. J. Biol. Chem. *270*, 22417–22421.
36. Eyckerman, S., Broekaert, D., Verhee, A., Vandekerckhove, J., and Tavernier, J. (2000). Identification of the Y985 and Y1077 motifs as SOCS3 recruitment sites in the murine leptin receptor. FEBS Lett. *486*, 33–37.
37. Koukos, G., Polytarchou, C., Kaplan, J.L., Morley-Fletcher, A., Gras-Miralles, B., Kokkotou, E., Baril-Dore, M., Pothoulakis, C., Winter, H.S., and Iliopoulos, D. (2013). MicroRNA-124 regulates STAT3 expression and is down-regulated in colon tissues of pediatric patients with ulcerative colitis. Gastroenterology *145*, 842–852.e2.
38. Hatziapostolou, M., Polytarchou, C., Aggelidou, E., Drakaki, A., Poultsides, G.A., Jaeger, S.A., Ogata, H., Karin, M., Struhl, K., Hadzopoulou-Cladaras, M., and Iliopoulos, D. (2011). An HNF4α-miRNA inflammatory feedback circuit regulates hepatocellular oncogenesis. Cell *147*, 1233–1247.
39. Sharma, S., Liu, J., Wei, J., Yuan, H., Zhang, T., and Bishopric, N.H. (2012). Repression of miR-142 by p300 and MAPK is required for survival signalling via gp130 during adaptive hypertrophy. EMBO Mol. Med. *4*, 617–632.
40. Sobotta, S., Raue, A., Huang, X., Vanlier, J., Jünger, A., Bohl, S., Albrecht, U., Hahnel, M.J., Wolf, S., Mueller, N.S., et al. (2017). Model Based Targeting of IL-6-Induced Inflammatory Responses in Cultured Primary Hepatocytes to Improve Application of the JAK Inhibitor Ruxolitinib. Front. Physiol. *8*, 775.
41. Lind, E.F., and Ohashi, P.S. (2014). Mir-155, a central modulator of T-cell responses. Eur. J. Immunol. *44*, 11–15.
42. Wilkinson, A.N., Gartlan, K.H., Kelly, G., Samson, L.D., Olver, S.D., Avery, J., Zomerdijk, N., Tey, S.K., Lee, J.S., Vuckovic, S., and Hill, G.R. (2018).

Granulocytes Are Unresponsive to IL-6 Due to an Absence of gp130. J. Immunol. *200*, 3547–3555.

43. Betz, U.A., and Müller, W. (1998). Regulated expression of gp130 and IL-6 receptor alpha chain in T cell maturation and activation. Int. Immunol. *10*, 1175–1184.
44. Radtke, S., Wüller, S., Yang, X.P., Lippok, B.E., Mütze, B., Mais, C., de Leur, H.S., Bode, J.G., Gaestel, M., Heinrich, P.C., et al. (2010). Cross-regulation of cytokine signalling: pro-inflammatory cytokines restrict IL-6 signalling through receptor internalisation and degradation. J. Cell Sci. *123*, 947–959.
45. Honke, N., Ohl, K., Wiener, A., Bierwagen, J., Peitz, J., Di Fiore, S., Fischer, R., Wagner, N., Wüller, S., and Tenbrock, K. (2014). The p38-mediated rapid down-regulation of cell surface gp130 expression impairs interleukin-6 signaling in the synovial fluid of juvenile idiopathic arthritis patients. Arthritis Rheumatol. *66*, 470–478.
46. Iwakawa, H.O., and Tomari, Y. (2015). The Functions of MicroRNAs: mRNA Decay and Translational Repression. Trends Cell Biol. *25*, 651–665.
47. Schumann, R.R., Kirschning, C.J., Unbehaun, A., Aberle, H.P., Knope, H.P., Lamping, N., Ulevitch, R.J., and Herrmann, F. (1996). The lipopolysaccharide-binding protein is a secretory class 1 acute-phase protein whose gene is transcriptionally activated by APRF/STAT/3 and other cytokine-inducible nuclear proteins. Mol. Cell. Biol. *16*, 3490–3503.
48. Xiao, Y., Wang, J., Yan, W., Zhou, Y., Chen, Y., Zhou, K., Wen, J., Wang, Y., and Cai, W. (2015). Dysregulated miR-124 and miR-200 expression contribute to cholangiocyte proliferation in the cholestatic liver by targeting IL-6/STAT3 signalling. J. Hepatol. *62*, 889–896.
49. Sonda, N., Simonato, F., Peranzoni, E., Calì, B., Bortoluzzi, S., Bisognin, A., Wang, E., Marincola, F.M., Naldini, L., Gentner, B., et al. (2013). miR-142-3p prevents macrophage differentiation during cancer-induced myelopoiesis. Immunity *38*, 1236–1249.
50. Kästingschäfer, C.S., Schäfer, S.D., Kiesel, L., and Götte, M. (2015). miR-142-3p is a novel regulator of cell viability and proinflammatory signalling in endometrial stroma cells. Reprod. Biomed. Online *30*, 553–556.
51. Chen, Y., Gao, D.Y., and Huang, L. (2015). In vivo delivery of miRNAs for cancer therapy: challenges and strategies. Adv. Drug Deliv. Rev. *81*, 128–141.
52. Kota, J., Chivukula, R.R., O'Donnell, K.A., Wentzel, E.A., Montgomery, C.L., Hwang, H.W., Chang, T.C., Vivekanandan, P., Torbenson, M., Clark, K.R., et al. (2009). Therapeutic microRNA delivery suppresses tumorigenesis in a murine liver cancer model. Cell *137*, 1005–1017.
53. Dhanasekaran, R., Gabay-Ryan, M., Baylot, V., Lai, I., Mosley, A., Huang, X., Zabludoff, S., Li, J., Kaimal, V., Karmali, P., and Felsher, D.W. (2017). Anti-miR-17 therapy delays tumorigenesis in MYC-driven hepatocellular carcinoma (HCC). Oncotarget *9*, 5517–5528.
54. Huang, X., Magnus, J., Kaimal, V., Karmali, P., Li, J., Walls, M., Prudente, R., Sung, E., Sorourian, M., Lee, R., et al. (2017). Lipid Nanoparticle-Mediated Delivery of Anti-miR-17 Family Oligonucleotide Suppresses Hepatocellular Carcinoma Growth. Mol. Cancer Ther. *16*, 905–913.
55. van Zandwijk, N., Pavlakis, N., Kao, S.C., Linton, A., Boyer, M.J., Clarke, S., Huynh, Y., Chrzanowska, A., Fulham, M.J., Bailey, D.L., et al. (2017). Safety and activity of microRNA-loaded minicells in patients with recurrent malignant pleural mesothelioma: a first-in-man, phase 1, open-label, dose-escalation study. Lancet Oncol. *18*, 1386–1396.
56. Palumbo, T., Poultsides, G.A., Kouraklis, G., Liakakos, T., Drakaki, A., Peros, G., Hatziapostolou, M., and Iliopoulos, D. (2016). A functional microRNA library screen reveals miR-410 as a novel anti-apoptotic regulator of cholangiocarcinoma. BMC Cancer *16*, 353.
57. Long, Z.W., Wu, J.H., Hong, C., Wang, Y.N., and Zhou, Y. (2018). MiR-374b Promotes Proliferation and Inhibits Apoptosis of Human GIST Cells by Inhibiting PTEN through Activation of the PI3K/Akt Pathway. Mol. Cells *41*, 532–544.
58. Xu, X., Wang, W., Su, N., Zhu, X., Yao, J., Gao, W., Hu, Z., and Sun, Y. (2015). miR-374a promotes cell proliferation, migration and invasion by targeting SRCIN1 in gastric cancer. FEBS Lett. *589*, 407–413.
59. Li, H., Chen, H., Wang, H., Dong, Y., Yin, M., Zhang, L., and Wei, J. (2018). MicroRNA-374a Promotes Hepatocellular Carcinoma Cell Proliferation by Targeting Mitogen-Inducible Gene-6 (MIG-6). Oncol. Res. *26*, 557–563.
60. Costa-Pereira, A.P., Tininini, S., Strobl, B., Alonzi, T., Schlaak, J.F., Is'harc, H., Gesualdo, I., Newman, S.J., Kerr, I.M., and Poli, V. (2002). Mutational switch of an IL-6 response to an interferon-gamma-like response. Proc. Natl. Acad. Sci. USA *99*, 8043–8047.
61. Rolvering, C., Zimmer, A.D., Kozar, I., Hermanns, H.M., Letellier, E., Vallar, L., Nazarov, P.V., Nicot, N., Ginolhac, A., Haan, S., et al. (2017). Crosstalk between different family members: IL27 recapitulates IFNγ responses in HCC cells, but is inhibited by IL6-type cytokines. Biochim Biophys Acta Mol Cell Res *1864*, 516–526.
62. Kaplan, D.H., Shankaran, V., Dighe, A.S., Stockert, E., Aguet, M., Old, L.J., and Schreiber, R.D. (1998). Demonstration of an interferon gamma-dependent tumor surveillance system in immunocompetent mice. Proc. Natl. Acad. Sci. USA *95*, 7556–7561.
63. Qin, Z., Kim, H.J., Hemme, J., and Blankenstein, T. (2002). Inhibition of methylcholanthrene-induced carcinogenesis by an interferon gamma receptor-dependent foreign body reaction. J. Exp. Med. *195*, 1479–1490.
64. Chen, X., Du, J., Jiang, R., and Li, L. (2018). MicroRNA-214 inhibits the proliferation and invasion of lung carcinoma cells by targeting JAK1. Am. J. Transl. Res. *10*, 1164–1171.
65. Yuan, J., Ji, H., Xiao, F., Lin, Z., Zhao, X., Wang, Z., Zhao, J., and Lu, J. (2017). MicroRNA-340 inhibits the proliferation and invasion of hepatocellular carcinoma cells by targeting JAK1. Biochem. Biophys. Res. Commun. *483*, 578–584.
66. Yu, D.L., Zhang, T., Wu, K., Li, Y., Wang, J., Chen, J., Li, X.Q., Peng, X.G., Wang, J.N., and Tan, L.G. (2017). MicroRNA-448 suppresses metastasis of pancreatic ductal adenocarcinoma through targeting JAK1/STAT3 pathway. Oncol. Rep. *38*, 1075–1082.
67. Zhang, Q., Huang, C., Yang, Q., Gao, L., Liu, H.C., Tang, J., and Feng, W.H. (2016). MicroRNA-30c Modulates Type I IFN Responses To Facilitate Porcine Reproductive and Respiratory Syndrome Virus Infection by Targeting JAK1. J. Immunol. *196*, 2272–2282.
68. Mukherjee, A., Di Bisceglie, A.M., and Ray, R.B. (2015). Hepatitis C virus-mediated enhancement of microRNA miR-373 impairs the JAK/STAT signaling pathway. J. Virol. *89*, 3356–3365.
69. Dunn, G.P., Koebel, C.M., and Schreiber, R.D. (2006). Interferons, immunity and cancer immunoediting. Nat. Rev. Immunol. *6*, 836–848.
70. Vainchenker, W., Leroy, E., Gilles, L., Marty, C., Plo, I., and Constantinescu, S.N. (2018). JAK inhibitors for the treatment of myeloproliferative neoplasms and other disorders. F1000Res. *7*, 82.
71. Cai, H., Liu, X., Zheng, J., Xue, Y., Ma, J., Li, Z., Xi, Z., Li, Z., Bao, M., and Liu, Y. (2017). Long non-coding RNA taurine upregulated 1 enhances tumor-induced angiogenesis through inhibiting microRNA-299 in human glioblastoma. Oncogene *36*, 318–331.
72. Liu, L., Chen, X., Zhang, Y., Hu, Y., Shen, X., and Zhu, W. (2017). Long non-coding RNA TUG1 promotes endometrial cancer development via inhibiting miR-299 and miR-34a-5p. Oncotarget *8*, 31386–31394.
73. Östling, P., Leivonen, S.K., Aakula, A., Kohonen, P., Mäkelä, R., Hagman, Z., Edsjö, A., Kangaspeska, S., Edgren, H., Nicorici, D., et al. (2011). Systematic analysis of microRNAs targeting the androgen receptor in prostate cancer cells. Cancer Res. *71*, 1956–1967.
74. Zheng, D., Dai, Y., Wang, S., and Xing, X. (2015). MicroRNA-299-3p promotes the sensibility of lung cancer to doxorubicin through directly targeting ABCE1. Int. J. Clin. Exp. Pathol. *8*, 10072–10081.
75. Wang, F., Dai, M., Chen, H., Li, Y., Zhang, J., Zou, Z., and Yang, H. (2018). Prognostic value of hsa-mir-299 and hsa-mir-7706 in hepatocellular carcinoma. Oncol. Lett. *16*, 815–820.
76. Zhang, J., Chong, C.C., Chen, G.G., and Lai, P.B. (2015). A Seven-microRNA Expression Signature Predicts Survival in Hepatocellular Carcinoma. PLoS ONE *10*, e0128628.
77. Lu, M., Kong, X., Wang, H., Huang, G., Ye, C., and He, Z. (2017). A novel microRNAs expression signature for hepatocellular carcinoma diagnosis and prognosis. Oncotarget *8*, 8775–8784.
78. Voorhees, P.M., Manges, R.F., Sonneveld, P., Jagannath, S., Somlo, G., Krishnan, A., Lentzsch, S., Frank, R.C., Zweegman, S., Wijermans, P.W., et al. (2013). A phase 2

multicentre study of siltuximab, an anti-interleukin-6 monoclonal antibody, in patients with relapsed or refractory multiple myeloma. Br. J. Haematol. *161*, 357–366.

79. San-Miguel, J., Bladé, J., Shpilberg, O., Grosicki, S., Maloisel, F., Min, C.K., Polo Zarzuela, M., Robak, T., Prasad, S.V., Tee Goh, Y., et al. (2014). Phase 2 randomized study of bortezomib-melphalan-prednisone with or without siltuximab (anti-IL-6) in multiple myeloma. Blood *123*, 4136–4142.

80. Orlowski, R.Z., Gercheva, L., Williams, C., Sutherland, H., Robak, T., Masszi, T., Goranova-Marinova, V., Dimopoulos, M.A., Cavenagh, J.D., Špička, I., et al. (2015). A phase 2, randomized, double-blind, placebo-controlled study of siltuximab (anti-IL-6 mAb) and bortezomib versus bortezomib alone in patients with relapsed or refractory multiple myeloma. Am. J. Hematol. *90*, 42–49.

81. Rossi, J.F., Négrier, S., James, N.D., Kocak, I., Hawkins, R., Davis, H., Prabhakar, U., Qin, X., Mulders, P., and Berns, B. (2010). A phase I/II study of siltuximab (CNTO 328), an anti-interleukin-6 monoclonal antibody, in metastatic renal cell cancer. Br. J. Cancer *103*, 1154–1162.

82. Dorff, T.B., Goldman, B., Pinski, J.K., Mack, P.C., Lara, P.N., Jr., Van Veldhuizen, P.J., Jr., Quinn, D.I., Vogelzang, N.J., Thompson, I.M., Jr., and Hussain, M.H. (2010). Clinical and Correlative Results of SWOG S0354: a Phase II Trial of CNTO328 (siltuximab), a Monoclonal Antibody against Interleukin-6, in Chemotherapy-Pretreated Patients with Castration-Resistant Prostate Cancer. Clin. Cancer Res. *16*, 3028–3034.

83. Fizazi, K., De Bono, J.S., Flechon, A., Heidenreich, A., Voog, E., Davis, N.B., Qi, M., Bandekar, R., Vermeulen, J.T., Cornfeld, M., and Hudes, G.R. (2012). Randomised phase II study of siltuximab (CNTO 328), an anti-IL-6 monoclonal antibody, in combination with mitoxantrone/prednisone versus mitoxantrone/prednisone alone in metastatic castration-resistant prostate cancer. Eur. J. Cancer *48*, 85–93.

84. Rossi, J.F., Lu, Z.Y., Jourdan, M., and Klein, B. (2015). Interleukin-6 as a therapeutic target. Clin. Cancer Res. *21*, 1248–1257.

85. Burger, R., Günther, A., Klausz, K., Staudinger, M., Peipp, M., Penas, E.M., Rose-John, S., Wijdenes, J., and Gramatzki, M. (2017). Due to interleukin-6 type cytokine redundancy only glycoprotein 130 receptor blockade efficiently inhibits myeloma growth. Haematologica *102*, 381–390.

86. Huang, E., Liu, R., and Chu, Y. (2015). miRNA-15a/16: as tumor suppressors and more. Future Oncol. *11*, 2351–2363.

87. Calin, G.A., Dumitru, C.D., Shimizu, M., Bichi, R., Zupo, S., Noch, E., Aldler, H., Rattan, S., Keating, M., Rai, K., et al. (2002). Frequent deletions and down-regulation of micro- RNA genes miR15 and miR16 at 13q14 in chronic lymphocytic leukemia. Proc. Natl. Acad. Sci. USA *99*, 15524–15529.

88. Klein, U., Lia, M., Crespo, M., Siegel, R., Shen, Q., Mo, T., Ambesi-Impiombato, A., Califano, A., Migliazza, A., Bhagat, G., and Dalla-Favera, R. (2010). The DLEU2/miR-15a/16-1 cluster controls B cell proliferation and its deletion leads to chronic lymphocytic leukemia. Cancer Cell *17*, 28–40.

89. Porkka, K.P., Ogg, E.L., Saramäki, O.R., Vessella, R.L., Pukkila, H., Lähdesmäki, H., van Weerden, W.M., Wolf, M., Kallioniemi, O.P., Jenster, G., and Visakorpi, T. (2011). The miR-15a-miR-16-1 locus is homozygously deleted in a subset of prostate cancers. Genes Chromosomes Cancer *50*, 499–509.

90. Lovat, F., Fassan, M., Gasparini, P., Rizzotto, L., Cascione, L., Pizzi, M., Vicentini, C., Balatti, V., Palmieri, D., Costinean, S., and Croce, C.M. (2015). miR-15b/16-2 deletion promotes B-cell malignancies. Proc. Natl. Acad. Sci. USA *112*, 11636–11641.

91. Wang, T., Hou, J., Li, Z., Zheng, Z., Wei, J., Song, D., Hu, T., Wu, Q., Yang, J.Y., and Cai, J.C. (2017). miR-15a-3p and miR-16-1-3p Negatively Regulate Twist1 to Repress Gastric Cancer Cell Invasion and Metastasis. Int. J. Biol. Sci. *13*, 122–134.

92. Feng, Q.Q., Dong, Z.Q., Zhou, Y., Zhang, H., and Long, C. (2018). miR-16-1-3p targets TWIST1 to inhibit cell proliferation and invasion in NSCLC. Bratisl. Lek Listy *119*, 60–65.

93. Liang, X.H., Hart, C.E., and Crooke, S.T. (2013). Transfection of siRNAs can alter miRNA levels and trigger non-specific protein degradation in mammalian cells. Biochim. Biophys. Acta *1829*, 455–468.

94. Saetrom, P., Heale, B.S., Snøve, O., Jr., Aagaard, L., Alluin, J., and Rossi, J.J. (2007). Distance constraints between microRNA target sites dictate efficacy and cooperativity. Nucleic Acids Res. *35*, 2333–2342.

95. Wilkens, L., Hammer, C., Glombitza, S., and Müller, D.E. (2012). Hepatocellular and cholangiolar carcinoma-derived cell lines reveal distinct sets of chromosomal imbalances. Pathobiology *79*, 115–126.

96. Ewald, F., Nörz, D., Grottke, A., Bach, J., Herzberger, C., Hofmann, B.T., Nashan, B., and Jücker, M. (2015). Vertical Targeting of AKT and mTOR as Well as Dual Targeting of AKT and MEK Signaling Is Synergistic in Hepatocellular Carcinoma. J. Cancer *6*, 1195–1205.

97. Kozomara, A., and Griffiths-Jones, S. (2014). miRBase: annotating high confidence microRNAs using deep sequencing data. Nucleic Acids Res. *42*, D68–D73.

98. Reczko, M., Maragkakis, M., Alexiou, P., Grosse, I., and Hatzigeorgiou, A.G. (2012). Functional microRNA targets in protein coding sequences. Bioinformatics *28*, 771–776.

99. Paraskevopoulou, M.D., Georgakilas, G., Kostoulas, N., Vlachos, I.S., Vergoulis, T., Reczko, M., Filippidis, C., Dalamagas, T., and Hatzigeorgiou, A.G. (2013). DIANA-microT web server v5.0: service integration into miRNA functional analysis workflows. Nucleic Acids Res. *41*, W169–W173.

100. Kirchmeyer, M., Servais, F.A., Hamdorf, M., Nazarov, P.V., Ginolhac, A., Halder, R., Vallar, L., Glanemann, M., Rubie, C., Lammert, F., Kreis, S., and Behrmann, I. (2018). Cytokine-mediated modulation of the hepatic miRNome: miR-146b-5p is an IL-6-inducible miRNA with multiple targets. J. Leukocyte Biol. *104*, 987–1002.

101. Haan, C., and Behrmann, I. (2007). A cost effective non-commercial ECL-solution for Western blot detections yielding strong signals and low background. J. Immunol. Methods *318*, 11–19.

OMTN, Volume *16*

Supplemental Information

Modulation of the IL-6-Signaling Pathway in Liver Cells by miRNAs Targeting gp130, JAK1, and/or STAT3

Florence A. Servais, Mélanie Kirchmeyer, Matthias Hamdorf, Nadège W.E. Minoungou, Stefan Rose-John, Stephanie Kreis, Claude Haan, and Iris Behrmann

Figure S1

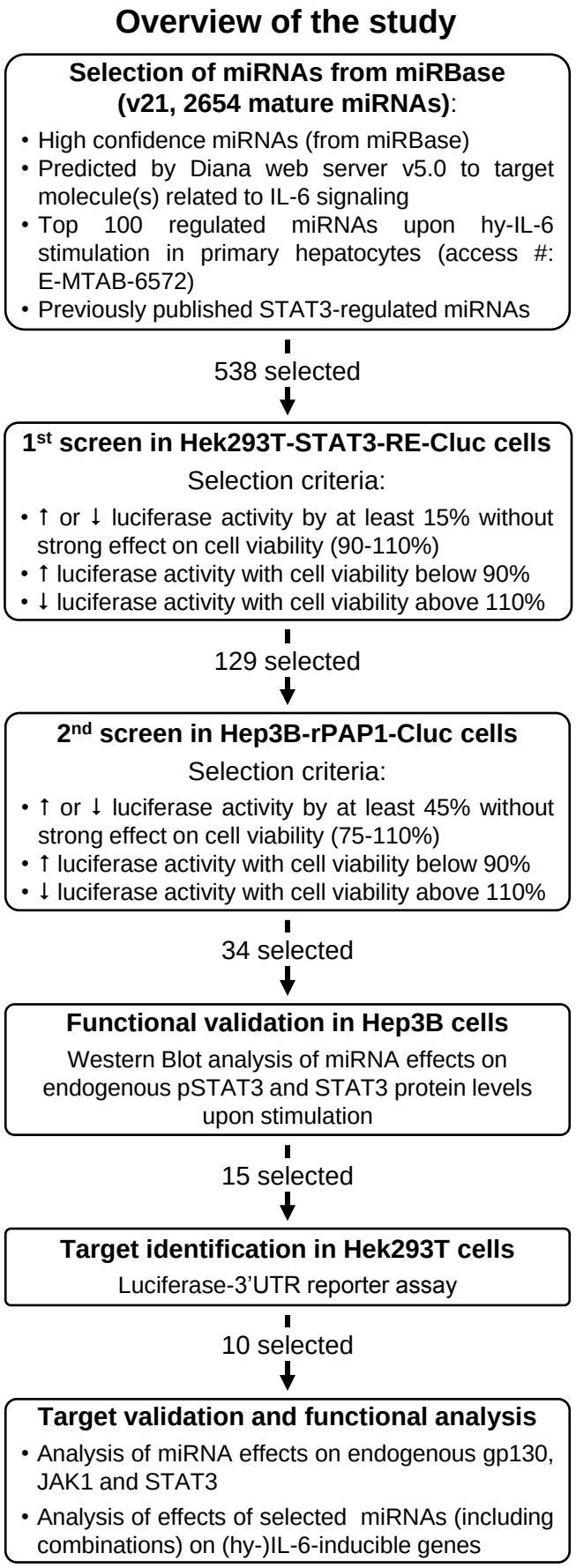
Overview of the study
Selection of miRNAs from miRBase (v21, 2654 mature miRNAs):
• High confidence miRNAs (from miRBase)
• Predicted by Diana web server v5.0 to target molecule(s) related to IL-6 signaling
• Top 100 regulated miRNAs upon hy-IL-6 stimulation in primary hepatocytes (access #: E-MTAB-6572)
• Previously published STAT3-regulated miRNAs
538 selected
1st screen in Hek293T-STAT3-RE-Cluc cells
Selection criteria:
• ↑ or ↓ luciferase activity by at least 15% without strong effect on cell viability (90-110%)
• ↑ luciferase activity with cell viability below 90%
• ↓ luciferase activity with cell viability above 110%
129 selected
2nd screen in Hep3B-rPAP1-Cluc cells
Selection criteria:
• ↑ or ↓ luciferase activity by at least 45% without strong effect on cell viability (75-110%)
• ↑ luciferase activity with cell viability below 90%
• ↓ luciferase activity with cell viability above 110%
34 selected
Functional validation in Hep3B cells
Western Blot analysis of miRNA effects on endogenous pSTAT3 and STAT3 protein levels upon stimulation
15 selected
Target identification in Hek293T cells
Luciferase-3'UTR reporter assay
10 selected
Target validation and functional analysis
• Analysis of miRNA effects on endogenous gp130, JAK1 and STAT3
• Analysis of effects of selected miRNAs (including combinations) on (hy-)IL-6-inducible genes

Figure S2

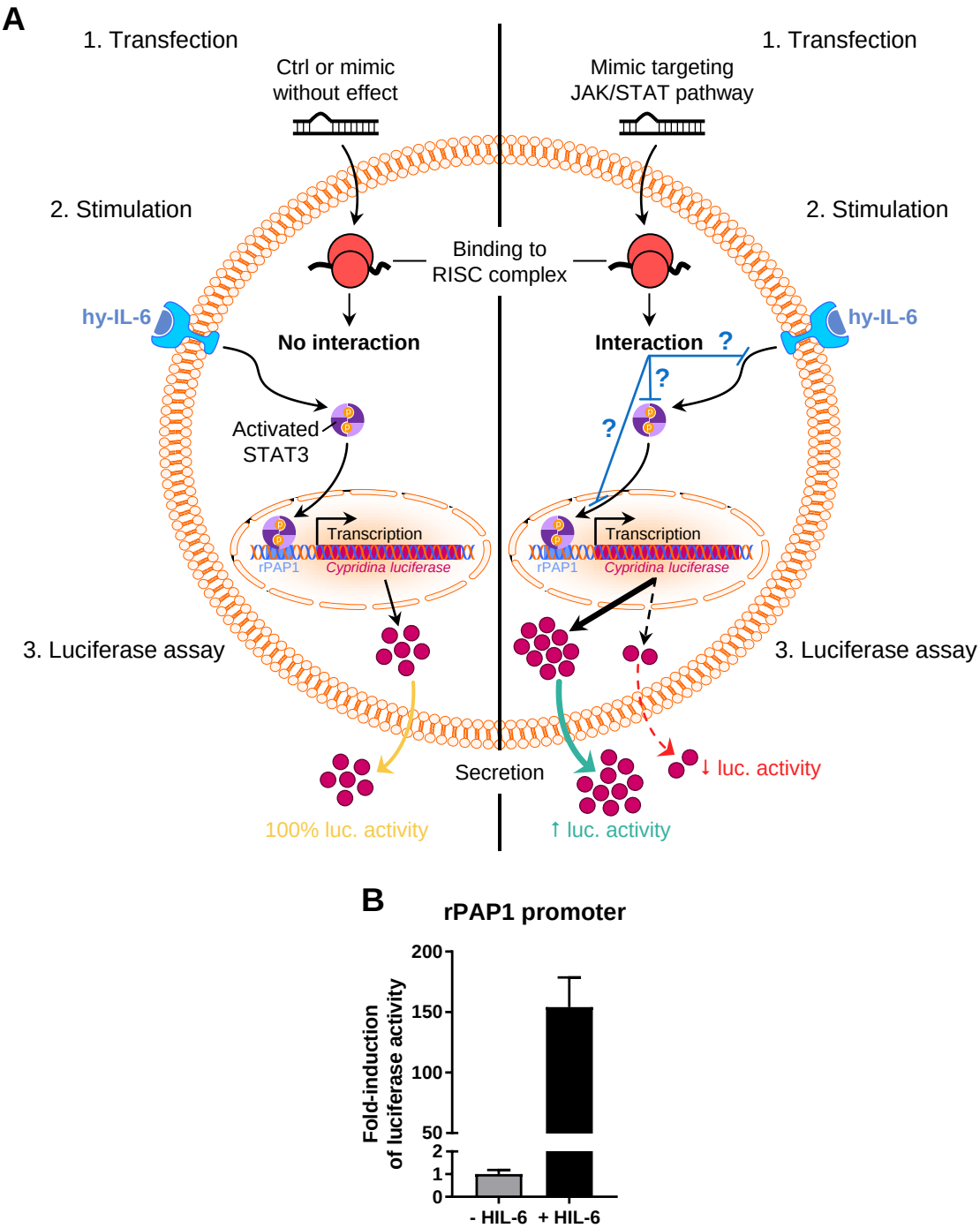

(**A**) Principle of the luciferase reporter assay. At day 1, cells were reverse transfected with a library of selected miRNA mimics (20 nM) and stimulated with 20 ng/mL hy-IL-6 at day 3. Upon stimulation, the secreted *Cypridina luciferase* gene is expressed in a STAT3-dependent manner. After 24 h, cell supernatants were collected and used for luciferase assay. **Left panel**: Some miRNA mimics as well as the negative control have no effect on the JAK/STAT3 signaling pathway, therefore a « normal » luciferase activity was measured in the supernatant of the cells. **Right panel**: Some mimics could have positive (e.g. by targeting negative regulators such as SOCS3) or negative effects (e.g. by targeting signaling molecules such as the receptor gp130) on the pathway, leading, respectively, to an increased or decreased luciferase activity measured. The STAT3-specific promoter rPAP1 was used for the screen performed in engineered Hep3B cells. (**B**) Fold induction of the luciferase activity measured in the supernatant of unstimulated and stimulated cells.

Figure S3

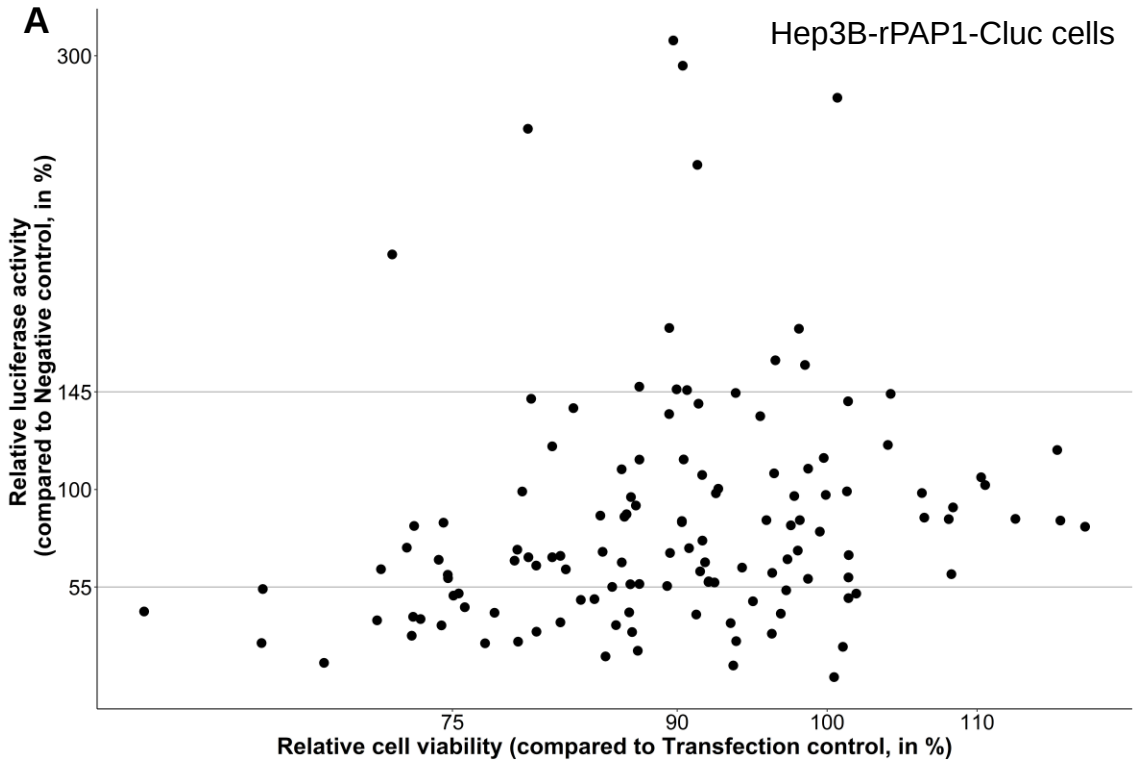

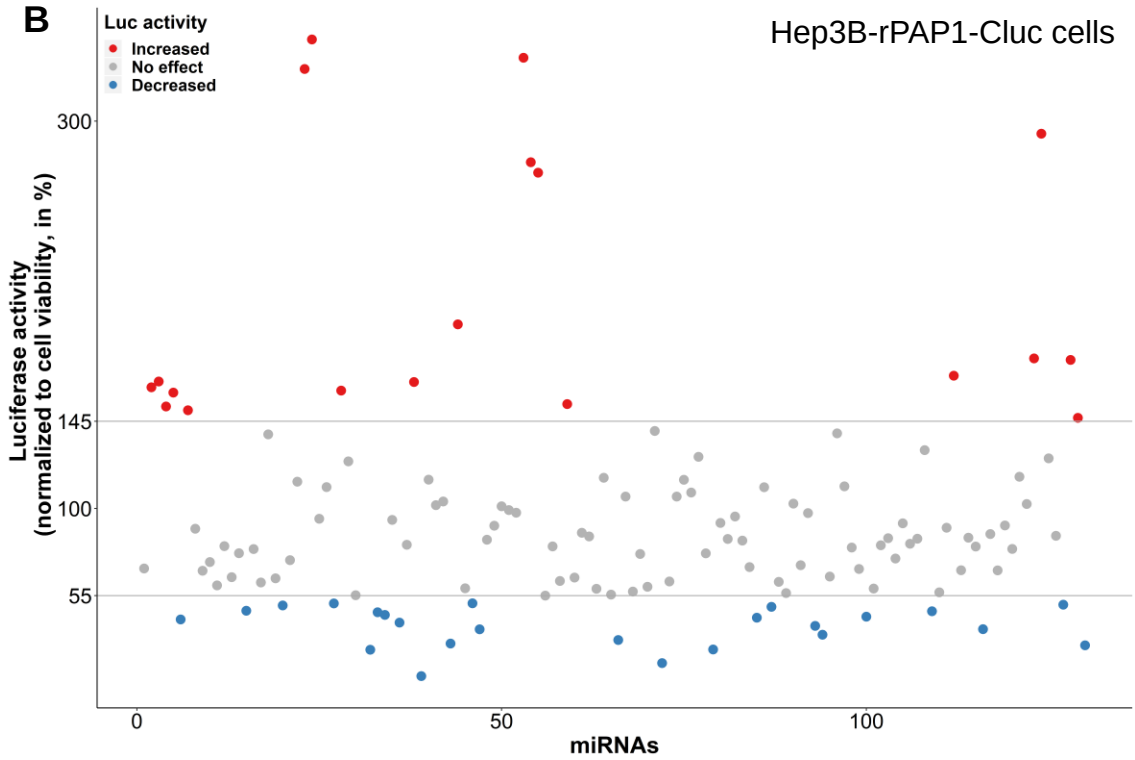

Screening results for the 129 selected candidate miRNAs in Hep3B-reporter cells (stably expressing the *Cypridina luciferase* gene under the control of the IL-6-inducible rPAP1 promoter). Cells were transfected with 20 nM mimics or Negative Control (NCM1) and stimulated with 20 ng/mL hy-IL-6 for 24 h. (**A**) (**Y axis**) Relative luciferase activity of transfected samples normalized to NCM1-transfected control samples. **(X axis)** Relative cell viability of transfected samples was determined with PrestoBlue, normalized to control samples with transfection reagent only. (**B**) The luciferase activity for each miRNA mimic was normalized to the associated viability. Dots represent the averaged luciferase activity obtained from 3 biological replicates. Some miRNA mimics reduced the level of pSTAT3 but were not further considered as they have been already associated with the JAK/STAT pathway (e.g. miR-17-5p targets STAT3 [He *et al.*, 2013]) or well-studied (e.g. miR-25-3p, reviewed in Sárközy *et* al., 2018, for its target genes and role in tumorigenesis).

Figure S4

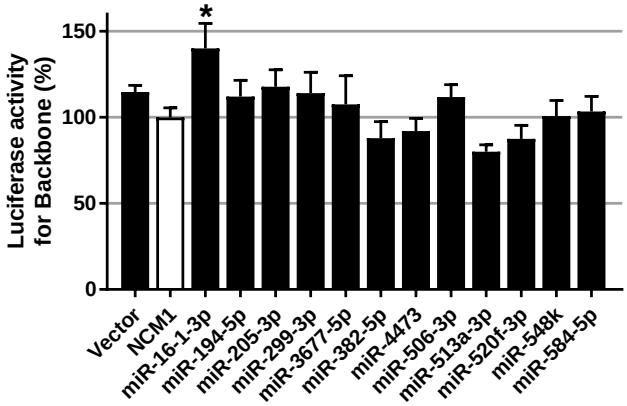

Hek293T cells were co-transfected with the selected mimics and the backbone vector harboring the *Gaussia luciferase* cDNA without 3'UTR inserted. Negative control mimic 1 (NCM1) is shown in white. Error bars represent standard deviation of 3 biological replicates. Kruskal-Wallis followed by Dunn's Post-Hoc test were performed to assess statistical significance represented with ⋆adjusted p-value <0.05. Refers to **Figures 2, 4** and **S7**.

Figure S5

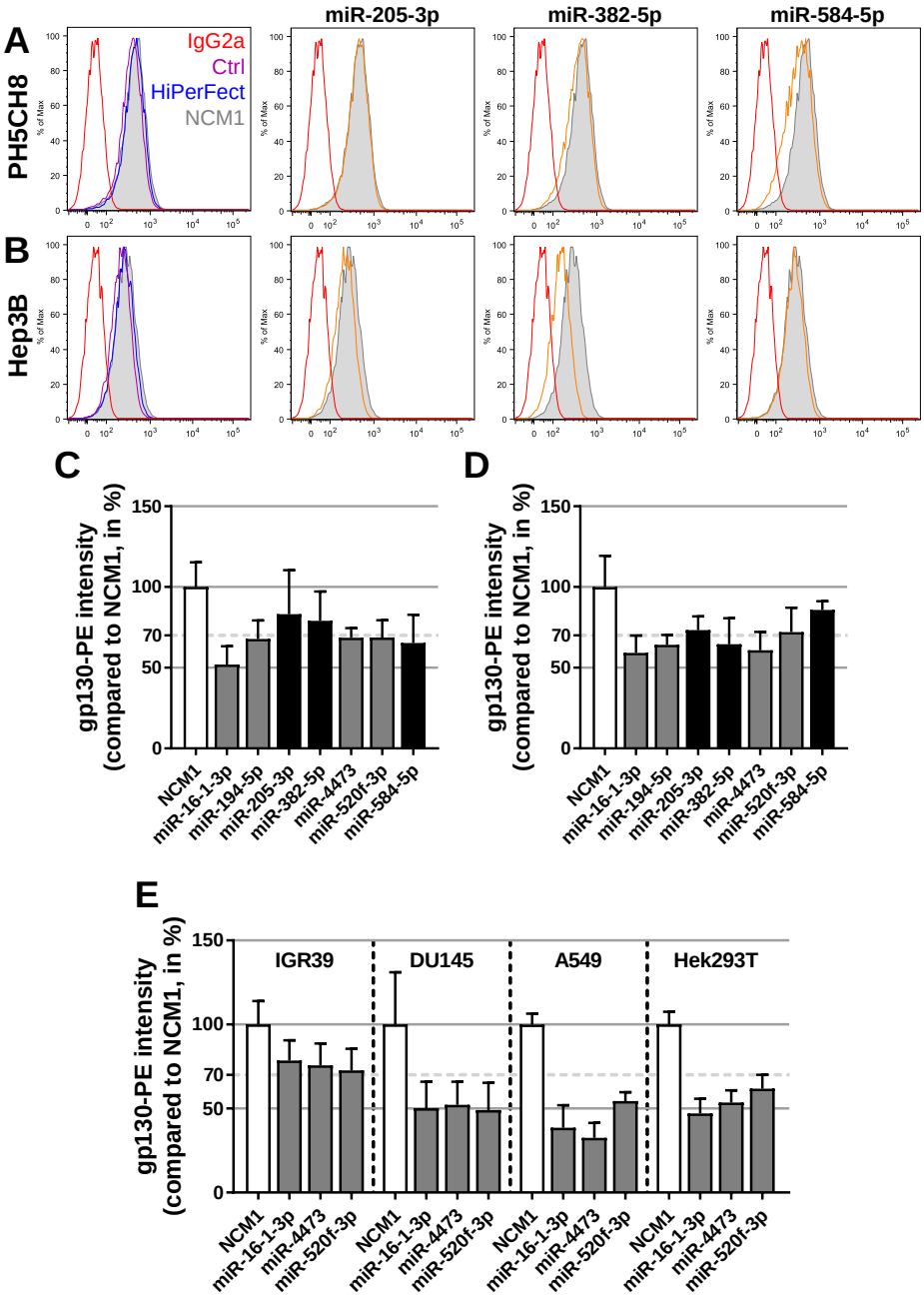

(**A**, **C**) Non-neoplastic PH5CH8 liver cells and (**B**, **D**) Hep3B hepatoma cells were either left untreated (Ctrl, in purple) or transfected with a negative control (NCM1, in gray) or one of the selected miRNA mimics and analyzed for gp130 expression level by flow cytometry. (**A-B**) Overlap. (**C-E**) Relative median of gp130-PE intensity in (**C**) PH5CH8, (**D**) Hep3B, and (**E**) in IGR39, DU145, A549, and HEK293T cells. Error bars represent the mean of 3 biological replicates. Refers to **Figures 2** and **6**.

Figure S6

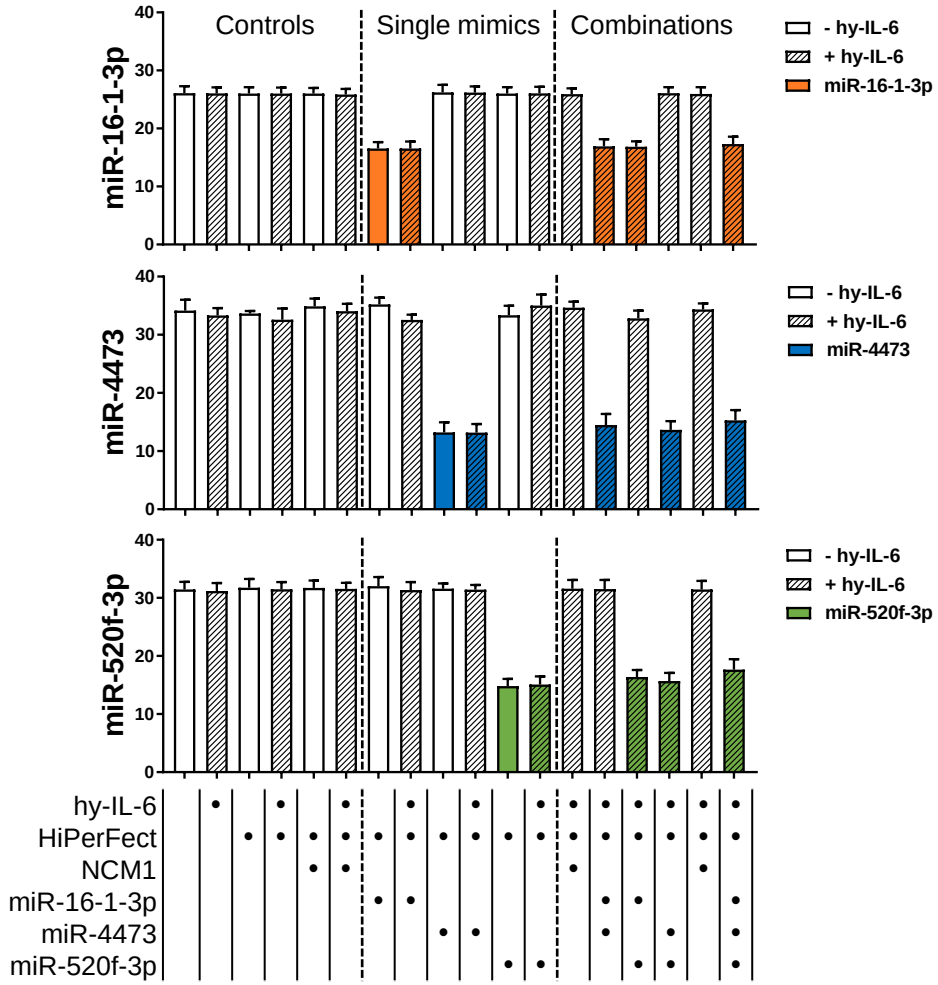

Expression levels of miR-16-1-3p, miR-4473 and/or miR-520f-3p upon reverse transfection of PH5CH8 cells with the corresponding mimics (represented by the Ct values obtained by qPCR; thus, successful transfection is reflected by reduced Ct values). Panel at the bottom indicates the applied treatments per lane. Refers to **Figure 3**.

Figure S7

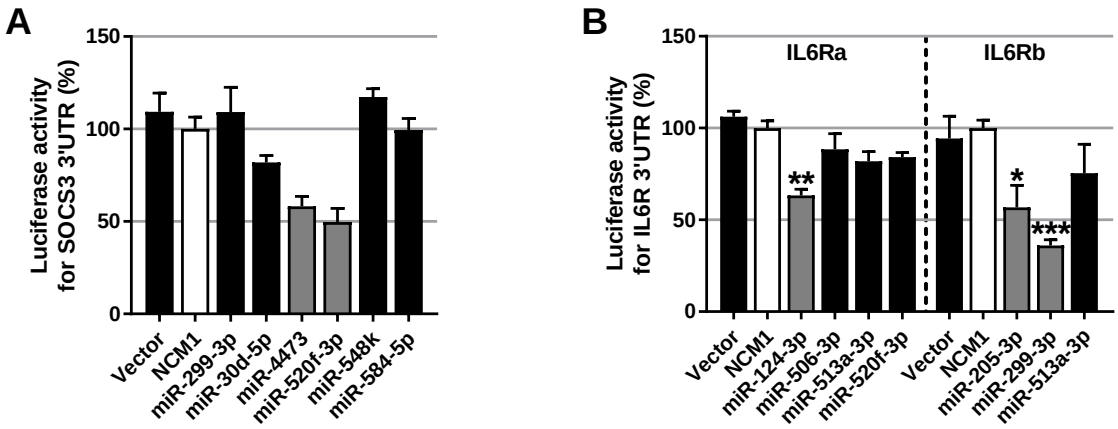

Hek293T cells were co-transfected with the selected mimics and the vectors harboring the *Gaussia luciferase* cDNA fused to the 3'UTR of (**A**) SOCS3 or (**B**) IL6R. Negative control mimic 1 (NCM1) is shown in white. Error bars represent standard deviation of 3 biological replicates. Kruskal-Wallis followed by Dunn's Post-Hoc test were performed to assess statistical significance represented with ⋆ adjusted p-value (adj.p.)<0.05, ⋆⋆adj.p.<0.01, ⋆⋆⋆ajd.p.<0.001. Refers to **Figure 6**.

Figure S8

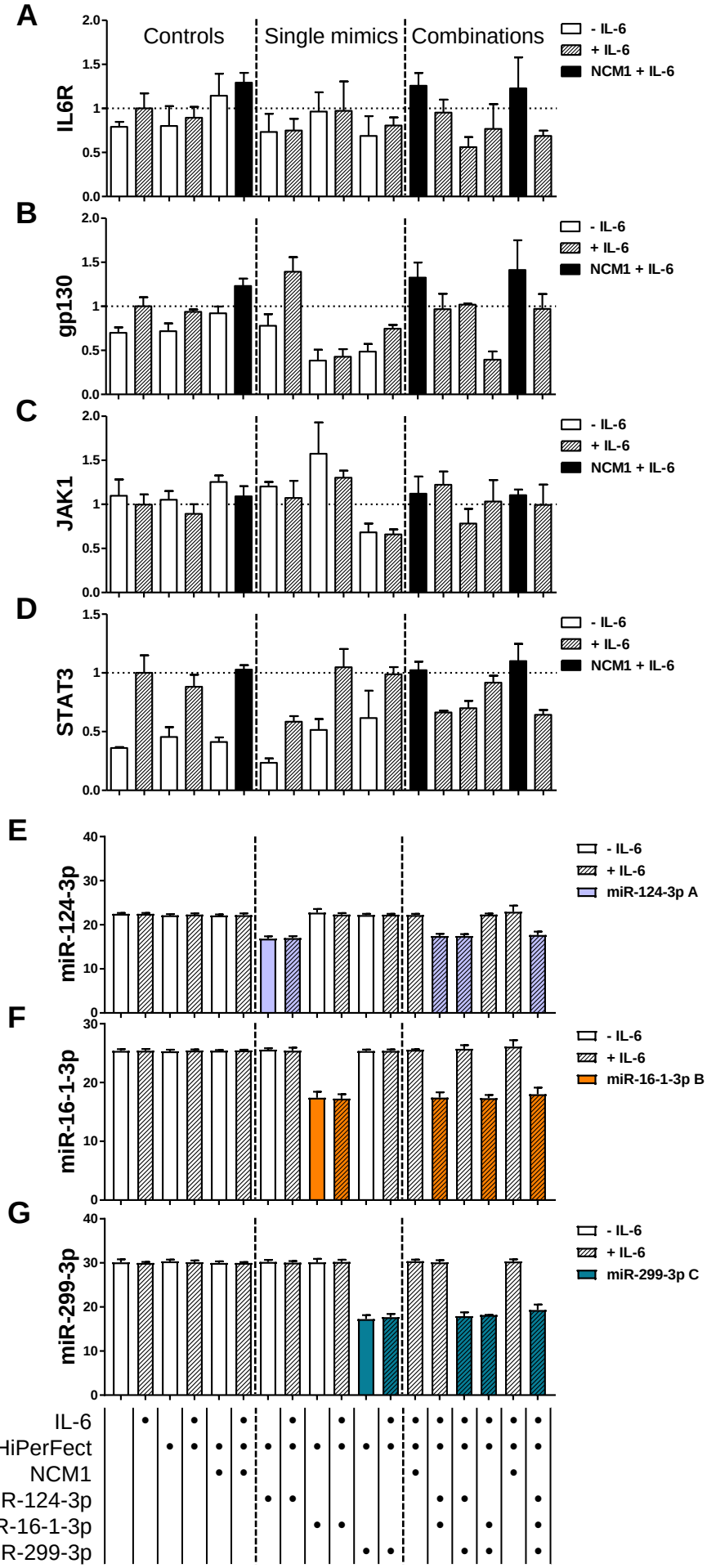

Expression levels of IL6R, gp130, JAK1, STAT3 (relative to IL-6 sample) as well as of miR-124-3p, miR-16-1-3p and /or miR-299-3p upon reverse transfection of Hep3B cells with the corresponding mimics (represented by the Ct values obtained by qPCR; thus, successful transfection is reflected by reduced Ct values). Panel at the bottom indicates the applied treatments per lane. Refers to **Figure 5**.

Table S1

List of all miRNAs present in the library.

538 human miRNA mimics were screened in Hek293T reporter cells.

miRNA	Accession #	miRNA	Accession #	miRNA	Accession #	miRNA	Accession #	miRNA	Accession #	miRNA	Accession #
let-7a-3p	MIMAT0004481	miR-1306-3p	MIMAT0005950	miR-181d-5p	MIMAT0002821	miR-219b-3p	MIMAT0019748	miR-3142	MIMAT0015011	miR-365	MIMAT0000710
let-7a-5p	MIMAT0000062	miR-1307-3p	MIMAT0005951	miR-182-5p	MIMAT0000259	miR-221-3p	MIMAT0000278	miR-3143	MIMAT0015012	miR-3652	MIMAT0018072
let-7b-5p	MIMAT0000063	miR-130a-3p	MIMAT0000425	miR-183-5p	MIMAT0000261	miR-221-5p	MIMAT0004568	miR-3144-5p	MIMAT0015014	miR-3656	MIMAT0018076
let-7d-5p	MIMAT0000065	miR-130a-5p	MIMAT0004593	miR-185-5p	MIMAT0000455	miR-222-3p	MIMAT0000279	miR-3148	MIMAT0015021	miR-3658	MIMAT0018078
let-7e-5p	MIMAT0000066	miR-130b-3p	MIMAT0000691	miR-186-5p	MIMAT0000456	miR-223-3p	MIMAT0000280	miR-3149	MIMAT0015022	miR-365b-5p	MIMAT0022833
let-7f-1-3p	MIMAT0004486	miR-1323	MIMAT0005795	miR-188-5p	MIMAT0000457	miR-22-3p	MIMAT0000077	miR-3150a-3p	MIMAT0015023	miR-3660	MIMAT0018081
let-7f-5p	MIMAT0000067	miR-132-3p	MIMAT0000426	miR-18a-5p	MIMAT0000072	miR-224-3p	MIMAT0009198	miR-3155a	MIMAT0015029	miR-3662	MIMAT0018083
let-7g-5p	MIMAT0000414	miR-133a-3p	MIMAT0000427	miR-18b-5p	MIMAT0001412	miR-224-5p	MIMAT0000281	miR-3158-3p	MIMAT0015032	miR-3671	MIMAT0018094
miR-100-5p	MIMAT0000098	miR-133b	MIMAT0000770	miR-1908-5p	MIMAT0007881	miR-23a-3p	MIMAT0000078	miR-31-5p	MIMAT0000089	miR-3677-5p	MIMAT0019221
miR-101-3p	MIMAT0000099	miR-1343-3p	MIMAT0019776	miR-190a-5p	MIMAT0000458	miR-23c	MIMAT0018000	miR-3163	MIMAT0015037	miR-3678-3p	MIMAT0018103
miR-103a-3p	MIMAT0000101	miR-134-5p	MIMAT0000447	miR-1910-3p	MIMAT0026917	miR-24-3p	MIMAT0000080	miR-3173-3p	MIMAT0015048	miR-3688-3p	MIMAT0018116
miR-105-5p	MIMAT0000102	miR-135a-5p	MIMAT0000428	miR-1912	MIMAT0007887	miR-2467-5p	MIMAT0019952	miR-3175	MIMAT0015052	miR-3689c	MIMAT0019007
miR-106a-5p	MIMAT0000103	miR-135b-5p	MIMAT0000758	miR-191-5p	MIMAT0000440	miR-25-3p	MIMAT0000081	miR-3185	MIMAT0015065	miR-3689d	MIMAT0019008
miR-106b-5p	MIMAT0000680	miR-136-5p	MIMAT0000448	miR-192-5p	MIMAT0000222	miR-26a-5p	MIMAT0000082	miR-3200-5p	MIMAT0017392	miR-369-3p	MIMAT0000721
miR-10a-5p	MIMAT0000253	miR-138-5p	MIMAT0000430	miR-193a-3p	MIMAT0000459	miR-26b-5p	MIMAT0000083	miR-320a	MIMAT0000510	miR-370-3p	MIMAT0000722
miR-10b-5p	MIMAT0000254	miR-139-5p	MIMAT0000250	miR-193b-3p	MIMAT0002819	miR-27a-3p	MIMAT0000084	miR-320b	MIMAT0005792	miR-371b-3p	MIMAT0019893
miR-1185-1-3p	MIMAT0022838	miR-1-3p	MIMAT0000416	miR-194-5p	MIMAT0000460	miR-27a-5p	MIMAT0004501	miR-320c	MIMAT0005793	miR-372-3p	MIMAT0000724
miR-1185-2-3p	MIMAT0022713	miR-141-3p	MIMAT0000432	miR-195-5p	MIMAT0000461	miR-27b-3p	MIMAT0000419	miR-320d	MIMAT0006764	miR-373-3p	MIMAT0000726
miR-1207-5p	MIMAT0005871	miR-141-5p	MIMAT0004598	miR-196a-5p	MIMAT0000226	miR-27b-5p	MIMAT0004588	miR-323a-3p	MIMAT0000755	miR-374a-3p	MIMAT0004688
miR-122-3p	MIMAT0004590	miR-142-3p	MIMAT0000434	miR-196b-5p	MIMAT0001080	miR-28-5p	MIMAT0000085	miR-32-3p	MIMAT0004505	miR-374a-5p	MIMAT0000727
miR-122-5p	MIMAT0000421	miR-142-5p	MIMAT0000433	miR-1972	MIMAT0009447	miR-2861	MIMAT0013802	miR-32-5p	MIMAT0000090	miR-374b-5p	MIMAT0004955
miR-1226-3p	MIMAT0005577	miR-143-3p	MIMAT0000435	miR-197-3p	MIMAT0000227	miR-296-5p	MIMAT0000690	miR-328-3p	MIMAT0000752	miR-376a-3p	MIMAT0000729
miR-124-3p	MIMAT0000422	miR-144-3p	MIMAT0000436	miR-199a-3p	MIMAT0000232	miR-299-3p	MIMAT0000687	miR-329-3p	MIMAT0001629	miR-376c-3p	MIMAT0000720
miR-124-5p	MIMAT0004591	miR-1469	MIMAT0007347	miR-199a-5p	MIMAT0000231	miR-29a-3p	MIMAT0000086	miR-330-3p	MIMAT0000751	miR-377-3p	MIMAT0000730
miR-1249-3p	MIMAT0005901	miR-146a-3p	MIMAT0004608	miR-199b-5p	MIMAT0000263	miR-29b-3p	MIMAT0000100	miR-331-3p	MIMAT0000760	miR-377-5p	MIMAT0004689
miR-1252-3p	MIMAT0026744	miR-146a-5p	MIMAT0000449	miR-19a-3p	MIMAT0000073	miR-29c-3p	MIMAT0000681	miR-335-3p	MIMAT0004703	miR-378a-3p	MIMAT0000732
miR-125a-5p	MIMAT0000443	miR-146b-5p	MIMAT0002809	miR-19b-3p	MIMAT0000074	miR-301a-3p	MIMAT0000688	miR-335-5p	MIMAT0000765	miR-378b	MIMAT0014999
miR-125b-1-3p	MIMAT0004592	miR-148a-3p	MIMAT0000243	miR-200a-3p	MIMAT0000682	miR-301b-3p	MIMAT0004958	miR-337-3p	MIMAT0000754	miR-378c	MIMAT0016847
miR-125b-5p	MIMAT0000423	miR-148b-3p	MIMAT0000759	miR-200b-3p	MIMAT0000318	miR-302a-3p	MIMAT0000684	miR-338-3p	MIMAT0000763	miR-378d	MIMAT0018926
miR-126-3p	MIMAT0000445	miR-149-3p	MIMAT0004609	miR-200c-3p	MIMAT0000617	miR-302c-5p	MIMAT0000716	miR-339-5p	MIMAT0000764	miR-378e	MIMAT0018927
miR-1269a	MIMAT0005923	miR-149-5p	MIMAT0000450	miR-202-3p	MIMAT0002811	miR-3065-5p	MIMAT0015066	miR-33a-5p	MIMAT0000091	miR-378f	MIMAT0018932
miR-1269b	MIMAT0019059	miR-150-5p	MIMAT0000451	miR-203a-3p	MIMAT0000264	miR-3074-3p	MIMAT0015027	miR-33b-5p	MIMAT0003301	miR-378h	MIMAT0018984
miR-1271-5p	MIMAT0005796	miR-151a-3p	MIMAT0000757	miR-204-5p	MIMAT0000265	miR-30a-5p	MIMAT0000087	miR-340-5p	MIMAT0004692	miR-378i	MIMAT0019074
miR-1273g-3p	MIMAT0022742	miR-152-3p	MIMAT0000438	miR-205-3p	MIMAT0009197	miR-30b-3p	MIMAT0004589	miR-342-3p	MIMAT0000753	miR-379-3p	MIMAT0004690
miR-1276	MIMAT0005930	miR-154-5p	MIMAT0000452	miR-208b-3p	MIMAT0004960	miR-30b-5p	MIMAT0000420	miR-345-3p	MIMAT0022698	miR-379-5p	MIMAT0000733
miR-1277-5p	MIMAT0022724	miR-155-5p	MIMAT0000646	miR-20a-5p	MIMAT0000075	miR-30c-2-3p	MIMAT0004550	miR-345-5p	MIMAT0000772	miR-381-3p	MIMAT0000736
miR-1278	MIMAT0005936	miR-15a-5p	MIMAT0000068	miR-20b-5p	MIMAT0001413	miR-30c-5p	MIMAT0000244	miR-34a-5p	MIMAT0000255	miR-382-5p	MIMAT0000737
miR-1281	MIMAT0005939	miR-15b-5p	MIMAT0000417	miR-210-3p	MIMAT0000267	miR-30d-5p	MIMAT0000245	miR-34b-3p	MIMAT0004676	miR-3911	MIMAT0018185
miR-128-3p	MIMAT0000424	miR-16-1-3p	MIMAT0004489	miR-2110	MIMAT0010133	miR-30e-5p	MIMAT0000692	miR-34c-5p	MIMAT0000686	miR-3915	MIMAT0018189
miR-1285-3p	MIMAT0005876	miR-16-5p	MIMAT0000069	miR-211-5p	MIMAT0000268	miR-3120-3p	MIMAT0014982	miR-3605-5p	MIMAT0017981	miR-3916	MIMAT0018190
miR-1287-5p	MIMAT0005878	miR-17-3p	MIMAT0000071	miR-2116-5p	MIMAT0011160	miR-3121-3p	MIMAT0014983	miR-3613-3p	MIMAT0017991	miR-3921	MIMAT0018196
miR-1290	MIMAT0005880	miR-17-5p	MIMAT0000070	miR-214-3p	MIMAT0000271	miR-3130-3p	MIMAT0014994	miR-3614-3p	MIMAT0017993	miR-3925-5p	MIMAT0018200
miR-129-5p	MIMAT0000242	miR-181a-2-3p	MIMAT0004558	miR-21-5p	MIMAT0000076	miR-3133	MIMAT0014998	miR-361-5p	MIMAT0000703	miR-3926	MIMAT0018201
miR-1296-5p	MIMAT0005794	miR-181a-5p	MIMAT0000256	miR-218-5p	MIMAT0000275	miR-3135a	MIMAT0015001	miR-362-3p	MIMAT0004683	miR-3928-3p	MIMAT0018205
miR-1304-5p	MIMAT0005892	miR-181b-3p	MIMAT0022692	miR-219a-1-3p	MIMAT0004567	miR-3135b	MIMAT0018985	miR-362-5p	MIMAT0000705	miR-409-3p	MIMAT0001639
miR-1305	MIMAT0005893	miR-181b-5p	MIMAT0000257	miR-219a-5p	MIMAT0000276	miR-3140-3p	MIMAT0015008	miR-363-3p	MIMAT0000707	miR-410-3p	MIMAT0002171

Table S1, continued

miRNA	Accession #	miRNA	Accession #	miRNA	Accession #	miRNA	Accession #	miRNA	Accession #	miRNA	Accession #
miR-411-5p	MIMAT0003329	miR-4687-3p	MIMAT0019775	miR-513c-3p	MIMAT0022728	miR-548b-5p	MIMAT0004798	miR-576-5p	MIMAT0003241	miR-4651	MIMAT0019715
miR-421	MIMAT0003339	miR-4700-5p	MIMAT0019796	miR-513c-5p	MIMAT0005789	miR-548c-3p	MIMAT0003285	miR-577	MIMAT0003242	miR-4659b-5p	MIMAT0019733
miR-422a	MIMAT0001339	miR-4707-3p	MIMAT0019808	miR-514a-3p	MIMAT0002883	miR-548c-5p	MIMAT0004806	miR-581	MIMAT0003246	miR-4668-3p	MIMAT0019746
miR-423-3p	MIMAT0001340	miR-4707-5p	MIMAT0019807	miR-514b-5p	MIMAT0015087	miR-548d-3p	MIMAT0003323	miR-582-5p	MIMAT0003247	miR-4669	MIMAT0019749
miR-424-3p	MIMAT0004749	miR-4725-3p	MIMAT0019844	miR-515-5p	MIMAT0002826	miR-548d-5p	MIMAT0004812	miR-583	MIMAT0003248	miR-512-3p	MIMAT0002823
miR-424-5p	MIMAT0001341	miR-4729	MIMAT0019851	miR-518a-5p	MIMAT0005457	miR-548e-3p	MIMAT0005874	miR-584-5p	MIMAT0003249	miR-513a-3p	MIMAT0004777
miR-425-5p	MIMAT0003393	miR-4731-3p	MIMAT0019854	miR-5193	MIMAT0021124	miR-548g-3p	MIMAT0005912	miR-587	MIMAT0003253	miR-513a-5p	MIMAT0002877
miR-4263	MIMAT0016898	miR-4734	MIMAT0019859	miR-5196-3p	MIMAT0021129	miR-548g-5p	MIMAT0022722	miR-589-5p	MIMAT0004799	miR-513b-5p	MIMAT0005788
miR-4270	MIMAT0016900	miR-4739	MIMAT0019868	miR-5197-3p	MIMAT0021131	miR-548h-3p	MIMAT0022723	miR-590-3p	MIMAT0004801	miR-548at-5p	MIMAT0022277
miR-4279	MIMAT0016909	miR-4755-3p	MIMAT0019896	miR-519a-3p	MIMAT0002869	miR-548h-5p	MIMAT0005928	miR-597-3p	MIMAT0026619	miR-548au-5p	MIMAT0022291
miR-4282	MIMAT0016912	miR-4755-5p	MIMAT0019895	miR-519c-3p	MIMAT0002832	miR-548i	MIMAT0005935	miR-601	MIMAT0003269	miR-548av-3p	MIMAT0022304
miR-4286	MIMAT0016916	miR-4763-3p	MIMAT0019913	miR-519d-3p	MIMAT0002853	miR-548j-5p	MIMAT0005875	miR-603	MIMAT0003271	miR-548aw	MIMAT0022471
miR-4298	MIMAT0016852	miR-4766-5p	MIMAT0019917	miR-519e-3p	MIMAT0002829	miR-548k	MIMAT0005882	miR-607	MIMAT0003275	miR-570-3p	MIMAT0003235
miR-4312	MIMAT0016864	miR-4775	MIMAT0019931	miR-519e-5p	MIMAT0002828	miR-548l	MIMAT0005889	miR-615-3p	MIMAT0003283	miR-5706	MIMAT0022500
miR-431-5p	MIMAT0001625	miR-4776-3p	MIMAT0019933	miR-520a-3p	MIMAT0002834	miR-548n	MIMAT0005916	miR-616-3p	MIMAT0004805	miR-574-3p	MIMAT0003239
miR-433-3p	MIMAT0001627	miR-4778-3p	MIMAT0019937	miR-520b	MIMAT0002843	miR-548o-3p	MIMAT0005919	miR-624-3p	MIMAT0004807	miR-576-3p	MIMAT0004796
miR-4418	MIMAT0018930	miR-4787-5p	MIMAT0019956	miR-520c-3p	MIMAT0002846	miR-548o-5p	MIMAT0022738	miR-625-5p	MIMAT0003294	miR-876-5p	MIMAT0004924
miR-4420	MIMAT0018933	miR-4793-3p	MIMAT0019966	miR-520d-3p	MIMAT0002856	miR-548p	MIMAT0005934	miR-627-5p	MIMAT0003296	miR-885-5p	MIMAT0004947
miR-4422	MIMAT0018935	miR-4793-5p	MIMAT0019965	miR-520e	MIMAT0002825	miR-548t-3p	MIMAT0022730	miR-628-5p	MIMAT0004809	miR-887-3p	MIMAT0004951
miR-4429	MIMAT0018944	miR-4796-3p	MIMAT0019971	miR-520f-3p	MIMAT0002830	miR-548t-5p	MIMAT0015009	miR-629-5p	MIMAT0004810	miR-92a-2-5p	MIMAT0004508
miR-4430	MIMAT0018945	miR-483-3p	MIMAT0002173	miR-522-3p	MIMAT0002868	miR-548v	MIMAT0015020	miR-638	MIMAT0003308	miR-92a-3p	MIMAT0000092
miR-4441	MIMAT0018959	miR-485-5p	MIMAT0002175	miR-526b-3p	MIMAT0002836	miR-548w	MIMAT0015060	miR-642a-5p	MIMAT0003312	miR-92b-3p	MIMAT0003218
miR-4451	MIMAT0018973	miR-487b-3p	MIMAT0003180	miR-532-3p	MIMAT0004780	miR-548x-3p	MIMAT0015081	miR-6503-5p	MIMAT0025462	miR-93-3p	MIMAT0004509
miR-4457	MIMAT0018979	miR-488-3p	MIMAT0004763	miR-539-5p	MIMAT0003163	miR-548x-5p	MIMAT0022733	miR-6511a-3p	MIMAT0025479	miR-9-3p	MIMAT0000442
miR-4459	MIMAT0018981	miR-490-3p	MIMAT0002806	miR-541-5p	MIMAT0004919	miR-548y	MIMAT0018354	miR-651-5p	MIMAT0003321	miR-941	MIMAT0004984
miR-4463	MIMAT0018987	miR-491-5p	MIMAT0002807	miR-542-3p	MIMAT0003389	miR-548z	MIMAT0018446	miR-652-3p	MIMAT0003322	miR-942-5p	MIMAT0004985
miR-4468	MIMAT0018995	miR-494-3p	MIMAT0002816	miR-543	MIMAT0004954	miR-550a-5p	MIMAT0004800	miR-654-5p	MIMAT0003330	miR-944	MIMAT0004987
miR-4473	MIMAT0019000	miR-495-3p	MIMAT0002817	miR-545-3p	MIMAT0003165	miR-550b-2-5p	MIMAT0022737	miR-660-5p	MIMAT0003338	miR-9-5p	MIMAT0000441
miR-4477a	MIMAT0019004	miR-497-3p	MIMAT0004768	miR-548a-3p	MIMAT0003251	miR-551b-3p	MIMAT0003233	miR-664b-3p	MIMAT0022272	miR-96-5p	MIMAT0000095
miR-4482-3p	MIMAT0020958	miR-497-5p	MIMAT0002820	miR-548a-5p	MIMAT0004803	miR-556-5p	MIMAT0003220	miR-664b-5p	MIMAT0022271	miR-98-5p	MIMAT0000096
miR-4492	MIMAT0019027	miR-499a-3p	MIMAT0004772	miR-548aa	MIMAT0018447	miR-5571-5p	MIMAT0022257	miR-671-5p	MIMAT0003880	miR-99a-5p	MIMAT0000097
miR-4508	MIMAT0019045	miR-499a-5p	MIMAT0002870	miR-548ab	MIMAT0018928	miR-5572	MIMAT0022260	miR-675-5p	MIMAT0004284	miR-99b-5p	MIMAT0000689
miR-450a-5p	MIMAT0001545	miR-5001-5p	MIMAT0021021	miR-548ac	MIMAT0018938	miR-5581-5p	MIMAT0022275	miR-708-5p	MIMAT0004926		
miR-450b-5p	MIMAT0004909	miR-500a-3p	MIMAT0002871	miR-548ae-3p	MIMAT0018954	miR-5582-3p	MIMAT0022280	miR-7-1-3p	MIMAT0004553		
miR-4514	MIMAT0019051	miR-5010-3p	MIMAT0021044	miR-548ah-3p	MIMAT0020957	miR-5583-3p	MIMAT0022282	miR-7-2-3p	MIMAT0004554		
miR-4516	MIMAT0019053	miR-5010-5p	MIMAT0021043	miR-548aj-3p	MIMAT0018990	miR-5584-3p	MIMAT0022284	miR-744-5p	MIMAT0004945		
miR-4517	MIMAT0019054	miR-502-5p	MIMAT0002873	miR-548aj-5p	MIMAT0022739	miR-559	MIMAT0003223	miR-758-3p	MIMAT0003879		
miR-451a	MIMAT0001631	miR-503-5p	MIMAT0002874	miR-548ak	MIMAT0019013	miR-5590-3p	MIMAT0022300	miR-7-5p	MIMAT0000252		
miR-452-3p	MIMAT0001636	miR-504-5p	MIMAT0002875	miR-548am-3p	MIMAT0019076	miR-561-3p	MIMAT0003225	miR-762	MIMAT0010313		
miR-4524a-3p	MIMAT0019063	miR-505-3p	MIMAT0002876	miR-548am-5p	MIMAT0022740	miR-5683	MIMAT0022472	miR-765	MIMAT0003945		
miR-4524a-5p	MIMAT0019062	miR-506-3p	MIMAT0002878	miR-548ap-5p	MIMAT0021037	miR-5688	MIMAT0022479	miR-766-3p	MIMAT0003888		
miR-4526	MIMAT0019065	miR-508-3p	MIMAT0002880	miR-548aq-3p	MIMAT0022264	miR-5691	MIMAT0022483	miR-767-3p	MIMAT0003883		
miR-4530	MIMAT0019069	miR-509-3-5p	MIMAT0004975	miR-548ar-3p	MIMAT0022266	miR-5692a	MIMAT0022484	miR-767-5p	MIMAT0003882		
miR-4536-5p	MIMAT0019078	miR-509-3p	MIMAT0002881	miR-548ar-5p	MIMAT0022265	miR-5692b	MIMAT0022497	miR-769-5p	MIMAT0003886		
miR-454-3p	MIMAT0003885	miR-509-5p	MIMAT0004779	miR-548as-3p	MIMAT0022268	miR-5692c	MIMAT0022476	miR-873-5p	MIMAT0004953		
miR-455-5p	MIMAT0003150	miR-510-5p	MIMAT0002882	miR-548as-5p	MIMAT0022267	miR-5693	MIMAT0022486	miR-874-3p	MIMAT0004911		

Table S2

Summary of the luciferase and PrestoBlue results obtained in the 1st and 2nd screens for each of the 34 miRNAs selected for functional analysis of their effects on STAT3 activation. Results represent the Luciferase or PrestoBlue signals measured, compared to the corresponding control and expressed in %. Errors (SD) represent standard deviation of 3 biological replicates.

miRNA	1st screen				2nd screen			
	Luciferase		PrestoBlue		Luciferase		PrestoBlue	
	% to Ctrl	SD	% to Ctrl	SD	% to Ctrl	SD	% to Ctrl	SD
let-7e-5p	126	18	107	13	157	8	99	1
let-7f-1-3p	66	30	103	9	34	9	81	10
miR-124-3p	**85**	**27**	**95**	**3**	**46**	**3**	**76**	**3**
miR-1277-5p	83	25	101	7	39	7	82	6
miR-130a-5p	80	9	100	1	43	7	87	6
miR-133a-3p	126	18	102	2	295	14	90	11
miR-133b	127	8	103	0	307	22	90	14
miR-142-3p	58	15	108	8	48	2	95	7
miR-155-5p	86	36	126	25	26	8	87	2
miR-16-1-3p	**72**	**33**	**104**	**9**	**23**	**5**	**85**	**12**
miR-17-5p	85	11	98	9	42	6	91	0
miR-188-5p	77	12	90	1	38	9	94	5
miR-193a-3p	117	15	100	2	160	24	97	5
miR-194-5p	**60**	**15**	**92**	**5**	**14**	**4**	**100**	**9**
miR-205-3p	**74**	**18**	**105**	**8**	**20**	**3**	**66**	**12**
miR-208b-3p	82	15	105	23	174	10	89	10
miR-25-3p	71	13	109	7	49	7	84	7
miR-299-3p	**67**	**15**	**103**	**8**	**30**	**6**	**79**	**12**
miR-30a-5p	141	7	105	6	266	43	80	4
miR-30c-5p	136	8	109	5	281	13	101	11
miR-30d-5p	**126**	**10**	**107**	**1**	**250**	**41**	**91**	**10**
miR-363-3p	72	20	104	7	49	12	84	6
miR-3677-5p	**136**	**20**	**105**	**21**	**43**	**15**	**78**	**7**
miR-382-5p	**84**	**11**	**90**	**13**	**30**	**5**	**94**	**15**
miR-4473	**74**	**35**	**117**	**4**	**19**	**7**	**94**	**17**
miR-494-3p	**77**	**17**	**97**	**1**	**27**	**6**	**101**	**25**
miR-506-3p	**74**	**8**	**99**	**1**	**37**	**6**	**86**	**11**
miR-513a-3p	**69**	**17**	**91**	**0**	**50**	**4**	**101**	**10**
miR-519e-5p	81	8	99	9	34	9	87	10
miR-520f-3p	**72**	**9**	**102**	**4**	**33**	**4**	**96**	**12**
miR-548k	**76**	**13**	**98**	**1**	**43**	**2**	**97**	**17**
miR-584-5p	**83**	**23**	**110**	**10**	**29**	**5**	**77**	**14**
miR-7-2-3p	81	13	92	14	174	12	98	6
miR-744-5p	117	15	92	10	208	95	71	12

Suppl. References:

He, M, Wang, QY, Yin, QQ, Tang, J, Lu, Y, Zhou, CX*, et al.* (2013). HIF-1alpha downregulates miR-17/20a directly targeting p21 and STAT3: a role in myeloid leukemic cell differentiation. *Cell Death Differ* **20**: 408-418.

Sárközy, M, Kahán, Z, and Csont, T (2018). A myriad of roles of miR-25 in health and disease. *Oncotarget* **9**: 21580-21612.